December 2023

Interaction of Technetium (IV) with Dibutyl Phosphate in n-Dodecane

Jonathan George
University of Nevada, Las Vegas

INTERACTION OF TECHNETIUM(IV) WITH DIBUTYL PHOSPHATE IN n-DODECANE

By

Jonathan George

Bachelor of Science – Chemistry
University of Nevada, Las Vegas
2019

A thesis submitted in partial fulfillment
of the requirements for the

Master of Science – Chemistry

Department of Chemistry and Biochemistry
College of Sciences
The Graduate College

University of Nevada, Las Vegas
December 2023

UNLV | GRADUATE COLLEGE

Thesis Approval

The Graduate College
The University of Nevada, Las Vegas

July 14, 2023

This thesis prepared by

Jonathan George

entitled

Interaction of Technetium (IV) with Dibutyl Phosphate in n-Dodecane

is approved in partial fulfillment of the requirements for the degree of

Master of Science – Chemistry
Department of Chemistry and Biochemistry

Frederic Poineau, Ph.D
Examination Committee Chair

Alyssa Crittenden, Ph.D.
Vice Provost for Graduate Education & Dean of the Graduate College

Artem Gelis, Ph.D.
Examination Committee Member

Kenneth Czerwinski, Ph.D.
Examination Committee Member

Alexander Barzilov, Ph.D.
Graduate College Faculty Representative

Abstract

During the reprocessing of nuclear fuel, the degradation of tributylphosphate (TBP) occurs as a result of radiolytic and thermal processes. These processes lead to the formation of minor amounts of dibutyl phosphate (HDBP). However, the presence of DBP poses a challenge in the partitioning of uranium (U), plutonium (Pu), and technetium (Tc) due to its chelating effects. The chelation of these elements by HDBP can interfere with their intended separation and purification, thereby impacting the efficiency and effectiveness of the reprocessing process. In this study, X-ray Absorption Fine Structure (XAFS) spectroscopy is employed to investigate the speciation of Tc following the extraction of Tc(IV) from both water (H_2O) and 1M nitric acid (HNO_3) using dibutyl phosphate (HDBP) in dodecane as the extracting system. The XAFS results revealed the formation of polymeric species containing Tc_2O_2 and Tc_2O units. Specifically, the species extracted from H_2O was proposed to have the formula $[Tc_2O_2(DBP{\cdot}HDBP)_4]$ (1), while the species extracted from 1M HNO_3 was proposed to have the formula $[Tc_2O(NO_3)_2(DBP)_2(DBP{\cdot}HDBP)_2]$ (2). The interatomic Tc-Tc distances in the Tc_2O_2 and Tc_2O units were found to be approximately 2.55(3) Å and 3.57(4) Å, respectively, resembling the distances observed in Tc(IV) dinuclear species. These findings suggest that the speciation of Tc(IV) in a HDBP/dodecane mixture involves the extraction of a species with a Tc_2O unit in the case of (2), while the species observed in (1) may be attributed to the re-dissolution of a Tc(IV)-DBP solid. The reduction kinetics of Tc(VII) with hydrazine were monitored through UV-Vis spectroscopy. Respective

concentrations in the aqueous and organic each phase was calculated using liquid scintillation counting.

Acknowledgements

I would like to express my gratitude to my mentors, colleagues, and parents who have played instrumental roles in my personal and professional journey. Their unwavering support, guidance, and encouragement have been invaluable, and I am deeply appreciative of their contributions.

First and foremost, I extend my sincere thanks to my mentors, Dr. Frederic Poineau and Dr. Artem Gelis, whose wisdom and expertise have shaped my growth and development. Their willingness to share their knowledge, offer constructive feedback, and provide invaluable insights have been pivotal in helping me navigate the challenges and opportunities I have encountered.

I am also immensely grateful to my colleagues, whose collaboration and camaraderie have made every step of this journey more enjoyable and fulfilling. Our discussions and their friendship have created a supportive and inspiring work environment that I am truly fortunate to be a part of.

Finally, I want to express my deepest appreciation to my parents. Their unconditional love, sacrifices, and unwavering belief in my abilities have been the bedrock upon which I have built my aspirations. Their encouragement and guidance have been a constant source of strength and motivation.

Table of Contents

Abstract iii

Acknowledgement v

Table of Contents vi

List of Tables viii

List of Figures ix

Chapter 1: Introduction 1

Chapter 2: Experimental Methods 5

2.1 Handling Technetium 5

2.2 Preparation of Technetium 5

2.3 Liquid-Liquid Extraction 6

2.4 EXAFS Sample Preparation 7

2.5 Instrumentation 9

2.5.1 UV-Vis Spectroscopy 9

2.5.2 Liquid Scintillation Counting 9

2.5.3 X-ray Absorption Fine Structure Spectroscopy 9

Chapter 3: Results and Discussion 11

3.1 Sample 1 11

3.1.1 Study of reaction in Sample....11

3.1.2 EXAFS – Sample 1....13

3.2 Sample 2....21

3.2.1 Study of reaction in Sample 2....21

3.2.2 EXAFS – Sample 2....23

3.3 Sample 1 and 2 Interpretations....29

Chapter 4: Conclusion and Future Work....33

Appendix....35

Bibliography....48

Curriculum Vita....54

List of Tables

Table 1 Solution parameters of single-cycle flow-sheet for the reprocessing of UNF from WWER-440.....3

Table 2 Experimental conditions for sample 1 and sample 2.....6

Table 3 EXAFS fit parameters obtained by fit of the k^3-EXAFS spectra for Sample 1. ΔE_0 = 6.17 eV. Reduced-chi^2 = 78.8. R = 9.56% 16

Table 4 Interatomic Tc-Tc and Tc-O(L) distances (Å) in Tc(IV) species with a Tc_2O_2 unit found by EXAFS (bold) and XRD.

.....18

Table 5 EXAFS fit parameters obtained by fit of the k^3-EXAFS spectra for Sample 2. ΔE_0 = 4.28 eV. Reduced-chi^2: 9.5. R = 5.64 %.....25

Table 6 Interatomic Tc-Tc and Tc-O(L) distances (Å) in Tc(IV) species with a Tc_2O unit found by EXAFS (bold) and XRD. 26

Table 7. Nature of species after extraction of M(IV) (M= Ce, Hf, Th, Pu) species with TBP from nitrate media.....30

List of Figures

Figure 1 a) Dibutylphosphoric acid. b) Dibutylphosphate dimer, $(DBP.HDBP)^-$, coordinated to a metal (M^{x+}). 2

Figure 2 UV-Vis spectra and time dependence of the reduction of 0.005M Tc(VII) in water using 1M hydrazine over 48 hours. 12

Figure 3 Reaction of TcO_4^- with N_2H_4 in H_2O at t=0 hours (left) and t=48 hours (right) 12

Figure 4 Fitted k^3-EXAFS spectra (top) and Fourier transform (bottom) of the k^3- EXAFS spectrum of Sample 1. Fit between k = 3 and 12.5 $Å^{-1}$. Experimental data in black and fit in red dots 15

Figure 5 Ball and stick representation of the $\{Tc_2O_2(PO_4)_4\}$ fragment (a) used for the EXAFS analysis of Sample 1. Color of atom: Tc in blue; O in red and P in orange. Tc0 represents the absorbing atom. 16

Figure 6 Ball and stick representation of the $[Tc_2O_2(DBP)_4(HDBP)_4]$ molecule. Color of atom: Tc in blue; O in red, C in dark grey, and P in orange. H atoms coordinated to C atoms are omitted for clarity. H atoms coordinated to O atoms are in light gray. 19

Figure 7 UV-Vis spectra and time dependence of the reduction of 0.005M Tc(VII) in 3M HNO_3 using 1M hydrazine over 48 hours. 20

Figure 8 Reaction of TcO_4^- with N_2H_4 in 1M HNO_3 at t=0 hours (left) and t=48 hours (right). 21

Figure 9 Fitted k^3-EXAFS spectra (top) and Fourier transform (bottom) of the k^3- EXAFS spectrum of Sample 2. Fit between k = 3 and 12.5 $Å^{-1}$. Experimental data in black and fit in red dots. 22

Figure 10 Ball and stick representation of the $\{Tc_2O(PO_4)_3(NO_3)\}$ fragment (b) used for the EXAFS analysis of Sample 2. Color of atom: Tc in blue; O in red, N in purple and P in orange. Tc0 represents the absorbing atom. 23

Figure 11 Ball and stick representation of the $[Tc_2O(NO_3)_2(DMP)_4(HDMP)_2]$ molecule. Color of atom: Tc in blue, O in red, C in grey, N in purple and P in orange. H atoms coordinated to C atoms are omitted for clarity. H atoms coordinated to O atoms are in light gray 27

Chapter 1: Introduction

Technetium (Tc), the first manmade element, has no stable isotopes. The two most common isotopes are ^{99m}Tc, an imaging agent used for medical diagnostics, and ^{99}Tc, a significant fission product of the nuclear industry[1]. The isotope ^{99}Tc is produced in a nuclear reactor (~2g / day for 100 MW of thermal energy) from the fission of ^{235}U. In the context of hydrometallurgical reprocessing of the used nuclear fuel (UNF), several separation processes (e.g., CoDCon [2]), like the PUREX process, have been considered[3]. PUREX is a separation process based on solvent extraction and utilizes tributyl phosphate (TBP, $(C_4H_9O)_3PO$) as the extracting agent in a kerosene diluent contacted with a nitric acid solution of UNF as the aqueous feeding phase. In these processes, Tc is a problematic element as it follows uranium (U) and plutonium (Pu) and interferes with several separation segments. Technetium can be found in both Pu/U streams, and in such, Tc affects the overall performance of the process. A detailed review of Tc chemistry in the PUREX process is presented in [4]. Another problematic species in the UNF reprocessing is dibutylphosphoric acid (HDBP, $(C_4H_9O)_2(OH)PO$, Figure 1a) a radiolytic and thermal degradation product of TBP [5,6]. Dibutylphosphate species can bind to metal ions as either the dibutylphosphate anion (DBP^-), dibutylphosphoric acid (HDBP), or as dibutylphosphate dimers ($DBP.HDBP^-$, Figure 1b) [7].

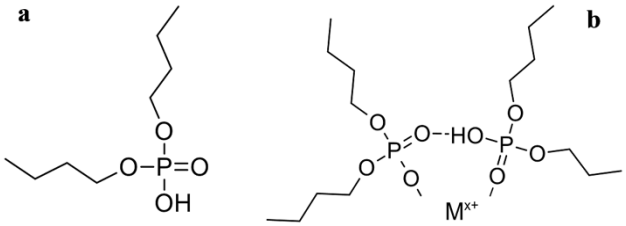

Figure 1. a) Dibutylphosphoric acid. b) Dibutylphosphate dimer, $(DBP.HDBP)^-$, coordinated to a metal (M^{x+}).

In a typical PUREX process, U(VI), Pu(IV) and Tc(VII) are initially extracted into the organic phase by TBP, then are separately back-extracted with a fresh aqueous phase to achieve partitioning. This separation step is based on the fact that the trivalent actinides form weaker complexes with TBP, and are not extracted under PUREX conditions, hence, converting Pu(IV) to Pu(III) with a suitable reducing agent (i.e. hydrazine, ferrous sulfamate, hydroxylamine amine, acetohydroxamic acid [8–10]) causes its stripping from the organic phase.

Several modifications of the PUREX process have been proposed in which parameters such as HNO_3 concentration, metal ion (U, Pu, Np, Tc) concentrations, and the nature of each reducing agent can vary. For example, the solution composition of the single-cycle flowsheet for the UNF reprocessing from WWER-440 reactor using N_2H_4 as the reducing agent is presented in **Table 1** [11].

Table 1. Solution parameters of single-cycle flow-sheet for the reprocessing of UNF from WWER-440.

Product	Solution composition				
	HNO_3, M	U, $g.L^{-1}$	Pu, $mg.mL^{-1}$	Np, $mg.mL^{-1}$	Tc, $mg.L^{-1}$ (mM)
Feed	3	210	2200	62	172 (1.74)
Raffinate	3.5	0.01	0.18	0.03	6.0 (0.06)
Extraction of U, Pu, Np, Tc	-	86	900	25	70 (0.71)
Pu and Tc strip product	1.5	0.03	4900	1.5	340 (3.43)

During this step, the behavior of Tc is poorly understood. In nitric acid, the heptavalent Tc may be reduced to lower valences (most likely IV) by various reducing agents [12–14]. Previous studies have shown that Tc(IV) species are not extractable by TBP but Tc(IV) can form kinetically stable complexes with DBP that can be extracted [15]. Solvent extraction studies have shown that a TcO^{2+} oxocation complex with the formula $TcO(DBP.HDBP)_2$ was extracted but no structural data has been reported. While the Tc-phosphine complexes have been widely studied [16,17], the coordination chemistry of

Tc-alkylphosphate species has been not reported yet. The coordination chemistry of second row transition metal alkylphosphates are also not well developed. In solution, research have primarily focused on the speciation of TBP species (Zr, Mo, Ru) that are relevant to separation processes [18–20]. In solid-state, research focused on the development of Zr layered materials that find applications in catalysis [21–23].

The study of Tc-DBP species gives the opportunity to investigate the coordination chemistry of the transition metal alkylphosphates as well as to better understand the behavior of Tc in UNF reprocessing chemistry. Here, for the first time, using XAFS spectroscopy, we examine the speciation of Tc-dibutylphosphate species in dodecane and discuss the formation mechanism of these species.

Chapter 2: Experimental Methods

2.1 Handling Technetium

Technetium-99 is a weak beta emitter with $E_{(max)}$ = 292 keV. All manipulations were performed in radiochemistry laboratories designed and approved for chemical synthesis using efficient HEPA-filtered fume hoods, and following UNLV's approved radioisotope handling and monitoring procedures. During manipulation of any solid technetium work, dosimeters, continuous air monitors, and quarterly bioassays were used to monitor the researcher's internal dose.

Solutions of technetium were prepared in either a 20mL glass scintillation vial or plastic 15mL centrifuge tube. During the reaction of technetium, nitric acid, and hydrazine, caps were left unsealed for a day inside the fume hood due to the explosive nature of the reaction. Extraction and centrifuging were done in a fume hood, in a tray, over an absorbent pad to prevent radiological contamination or spills. For spectroscopic and counting methods, preparation was done inside a radiation laboratory, inside a fume hood, labeled, and sealed before entering the spectrophotometer and LSC areas.

2.2 Preparation of Technetium

The technetium starting material, ammonium pertechnetate (NH_4TcO_4), was purchased from Oak Ridge National Lab and treated with H_2O_2 to oxidize any reduced forms of Tc [24]. Standardization of prepared aqueous NH_4TcO_4 solutions were conducted according to an established procedure [25]. Solid $KTcO_4$ was obtained after dissolution of NH_4TcO_4 in water and precipitation with an aqueous KOH solution. A $KTcO_4$ stock solution (0.107 M) was prepared by dissolving solid KTcO4 in water (18.2 MΩ).

2.3 Liquid-Liquid Extraction

Liquid-liquid extraction was employed for the separation and purification of reduced technetium (IV) species. For this extraction, a solvent mixture of 30% v/v HDBP in n-dodecane has been investigated. The HDBP and n-dodecane, with purities of 97% and 99% respectively, were acquired from Sigma Aldrich without further purification. A previous study has shown that the main impurity in HDBP (97 % from Sigma-Aldrich) is TBP (~2%) [26].The concentration of technetium in the organic phase was calculated from the difference in the aqueous phase before and after extraction seen in **Table 2**.

Table 2. Experimental conditions for sample 1 and sample 2.

	Sample 1	Sample 2
Aq. media reduction	H_2O	1 M HNO_3
Aq. media extraction	H_2O	1 M HNO_3
Organic media	HDBP 30% (v/v) in dodecane	HDBP 30% (v/v) in dodecane
$[Tc]_{aq}$ before extraction (mM)	4.99	4.99
$[Tc]_{aq}$ after extraction (mM)	0.01	0.51
$[Tc]_{org}$* (mM)	4.98	4.48

*Calculated by difference: $[Tc]_{org} = [Tc]_{aq\ before\ extraction} - [Tc]_{aq\ after\ extraction}$

2.4 EXAFS Sample preparation

Sample 1 was prepared without the addition of HNO3. A suspension of $TcO_2 \cdot xH_2O$ in water (3 mL) was prepared using the literature method [27]. Deionized water (2.767 mL) and an aliquot of the KTcO4 stock solution (140 µL, 0.01498 mmol) were added in a vial. Then, hydrazine (93 µl, 2.90 mmol) was added to the vial. After the addition of hydrazine, an intense brown color was observed, and the vial left

undisturbed in the hood with the cap open. After a day at room temperature (RT), a brown suspended solid ($TcO_2 \cdot xH_2O$) was observed. For the extraction, the same volume (3 mL) of the 30% by volume solution of HDBP in n-dodecane was added to the $TcO_2 \cdot xH_2O$ aqueous suspension. The tube was vortexed and centrifuged for splitting phases. A sample of the organic phase was collected for analysis by XAFS spectroscopy. The XANES analysis of the spectra (**Figure S2**), using the first derivative method, indicates an edge position of 21055.1 eV which is in agreement with the presence of Tc(IV) [28]. Sample 1 was analyzed by UV-visible spectroscopy and its spectrum exhibits bands at 380 and 510 nm (**Figure S3**).

Sample 2 was prepared in ~1M nitric acid in a similar manner to Sample 1 using a method that produces Tc(IV) with an unknown structure [29]. An aliquot of the KTcO4 stock solution (140 µL) was diluted with 1M HNO3 (2.767 mL), then, hydrazine (93 µL) was added, and the vial left undisturbed at RT. After a day, when a brown solution was observed, extraction with HDBP/n-dodecane (30 % by volume) was performed in similar manner as above. After splitting phases, the aliquot of organic phase was collected and analyzed by XAFS spectroscopy. The analysis of the XANES spectrum (**Figure S4**), using the first derivative method, indicates an edge position of 21055.2 eV which is in agreement with the presence of Tc(IV). Sample 2 was analyzed by UV-visible spectroscopy and its spectrum exhibits bands at 370 nm and 499 nm (**Figure S5**).

2.5 Instrumentation

2.5.1 Ultraviolet Visible Spectroscopy

UV-Vis(Ultraviolet-Visible) measurements were performed using a Varian Cary 50 Scan UV spectrophotometer in Starna Cells 9-Q-10-GL14-C (1.4mL, 1cm, screw cap quartz) cuvette at room temperature. The instrument was used in a single beam mode using a blank reference solution for baseline correction. Measurements were taken from 800nm to 200nm. Kinetic measurements were done by placing a cuvette with a Tc containing solution and monitoring the region at 400nm over the period of a day (**Figure S1**).

2.5.2 Liquid Scintillation Counting

Liquid Scintillation measurements were performed on a Beckman LS 6000 LSC (liquid scintillation counter) with a β_{eff} of 66.3%. Aqueous technetium samples (10μL) were loaded into the LSC cocktail (10mL) and shaken vigorously. A specific activity of 630 $Bq/\mu g_{Tc}$ was used [30]. Count times ranged from 1-10 minutes to achieve a β% error less than one.

2.5.3 X-ray Absorption Fine Structure Spectroscopy

XAFS measurements of samples were performed at the Argonne National Laboratory Advanced Photon Source at the BESSRC-CAT 12 BM-B station. The technetium sample (~18 μL) was placed in a Teflon NMR tube insert holder and covered with Kapton film. XAFS spectra were recorded at the Tc-K edge (21,044 eV) in fluorescence mode at room temperature using a 13 elements germanium detector. A

double crystal of Si [1 1 1] was used as a monochromator. The energy steps were 0.6eV in the XANES region and 0.05 Å-1 in the EXAFS region. The energy was calibrated using a molybdenum foil (Mo-K edge = 20,000 eV). Six spectra were recorded in the 0-15 Å-1 k range and averaged.

For the set of data, the EXAFS spectra were extracted using the Athena software [31] and data analysis was performed using Winxas [32]. For the fitting procedure, amplitude and phase shift functions were calculated by FEFF 8.2 [33]. Input files were generated by Atoms [34] within Artemis. The uncertainty on the distances and coordination numbers found by EXAFS are respectively 1% and 25% [35]. Molecular representations were performed using the Avogadro software [36].

Chapter 3: Results and Discussions

3.1 Sample 1

3.1.1 Study of reaction in Sample 1

The reaction between TcO_4^- and N_2H_4 in H_2O ([Tc] = 0.005M, [N_2H_4] = 1M) was monitored for 48 hours by UV-Vis spectroscopy in Figure **2**. A blank sample of H_2O was used as the background. The formation of the band at 400nm rises for the first six hours. Afterwards, the signal drops dramatically following 48 hours. The decrease is due to Tc(IV) precipitating out of solution in the form of TcO_2. In **Figure 3**, a pink solution is noticed when adding N_2H_4 to solution. After the reaction is complete, a clear solution is observed with a black suspension.

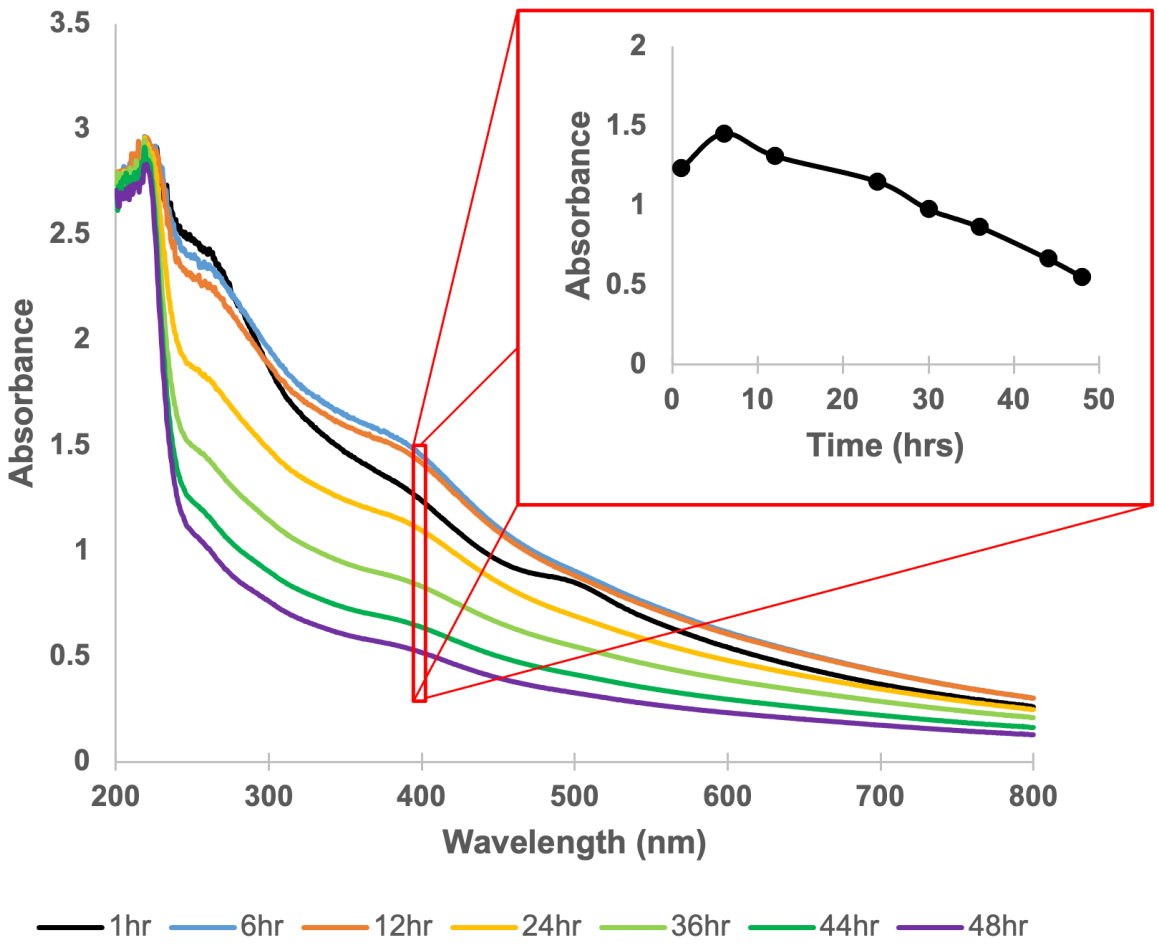

Figure 2. UV-Vis spectra and time dependence of the reduction of 0.005M Tc(VII) in water using 1M hydrazine over 48 hours.

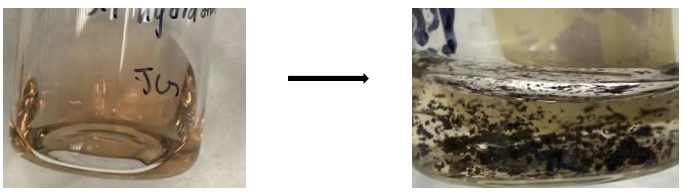

Figure 3. Reaction of TcO_4^- in with N_2H_4 in H_2O at t=0 hours (left) and t=48 hours (right).

3.1.2 EXAFS – Sample 1

The EXAFS spectrum of Sample 1 was averaged, k^3-weighed and the Fourier transform (FT) performed in the 3-12.5 $Å^{-1}$ k range. The FT graph (Figure 1) shows three main peaks: Peak A centered at R + Δ ~ 1.65 Å, Peak B at ~ 2.20 Å and Peak C at ~ 3.05 Å. The position of peak A is similar to the one found for Tc(IV) species with Tc-O bonds and likely to indicate the presence of O atoms in the first coordination sphere of the absorbing Tc atom. For example, the peak characteristic of the Tc-O contribution on the FT of $TcO_2 \cdot xH_2O$ is centered at R + Δ ~ 1.7 Å [37].

Peak B has an intense magnitude and might be caused by the presence of Tc atoms in the second coordination sphere of the absorbing atom. The FT of Sample 1 in the 1-2.8 Å domain is similar to the one for Tc species with Tc_2O_2 unit. Peak B was analyzed by Fourier filtering using the Tc-Tc scattering path calculated in TcO_2 [38]. A window filter was performed on the FT between R + □ = [1.65 - 2.45] Å. The FT was back-transformed and the fit conducted using the Tc-Tc scattering path. The Debye-Waller Factor (DWF, □^{2}, given in $Å^2$) was fixed to the one reported for the Tc-Tc contribution in $TcO_2.xH_2O$ (0.0030)[39] and all the other parameters were allowed to vary. The result of the fit (**Figure S6, Table S1**) supports the presence of 0.7(2) Tc atoms at 2.57(3) Å. Peak C is also characteristic of atoms in the second coordination sphere and is due to Tc-P scatterings from [DBP] units coordinated to the Tc atom. This hypothesis indicates that Sample 1 would contain a dinuclear species with a Tc_2O_2 unit coordinated to [DBP] units.

In order to evaluate this hypothesis, the EXAFS spectrum was fitted using the scattering paths calculated in a putative $\{Tc_2O_2(PO_4)_4\}$ fragment (a) (**Figure 5**). The

fragment (a) was constructed using the {Tc-O-P} and {Tc_2O_2} metrics extracted from [$TcCl_4(TPPO)_2$][40] and [$Tc_2O_2(HEDTA)_2.6H_2O$][41] respectively. The acronyms TPPO and HEDTA stand for triphenylphosphine oxide and hydroxyethyl-ethylenediaminetriacetic acid, respectively.

For the fit, the Tc0-Oa, Tc0-Ob, Tc0-Tca and Tc0-P (SS1) single-scattering paths and the Tc0-Ob-P (MS1) multi-scattering paths were used. The DWF for the Tc0-OA, Tc0-OB and the Tc0-Tca scattering path were fixed to the one reported in the literature for $TcO_2 \cdot xH_2O$ (Tc0-Oa: 0.003, Tc0-Ob: 0.006, Tc0-Tca: 0.003) [32]. For the SS1 scattering path, the DWF was fixed to 0.006, a value similar the one found for the U-P scattering path in $UO_2(NO_3) \cdot 2TBP$ (0.0054) [42]. For MS1 and SS1, the value of the C.N were correlated (i.e., $C.N_{MS1} = 2.\ C.N_{SS1}$). The ΔE_0 was constrained to be the same value for each scattering path; all the other parameters were allowed to vary. The results of the fit (**Figure 4, Table 2**) indicate the environment of the absorbing atom to be constituted by 0.5(1) Oa atoms at 1.84(2) Å, 4.3 ± 1.0 Ob atoms at 2.07(2) Å, 0.7(2) Tc atom at 2.55(3) Å and 5.0 ± 1.2 P atoms at 3.39(3) Å.

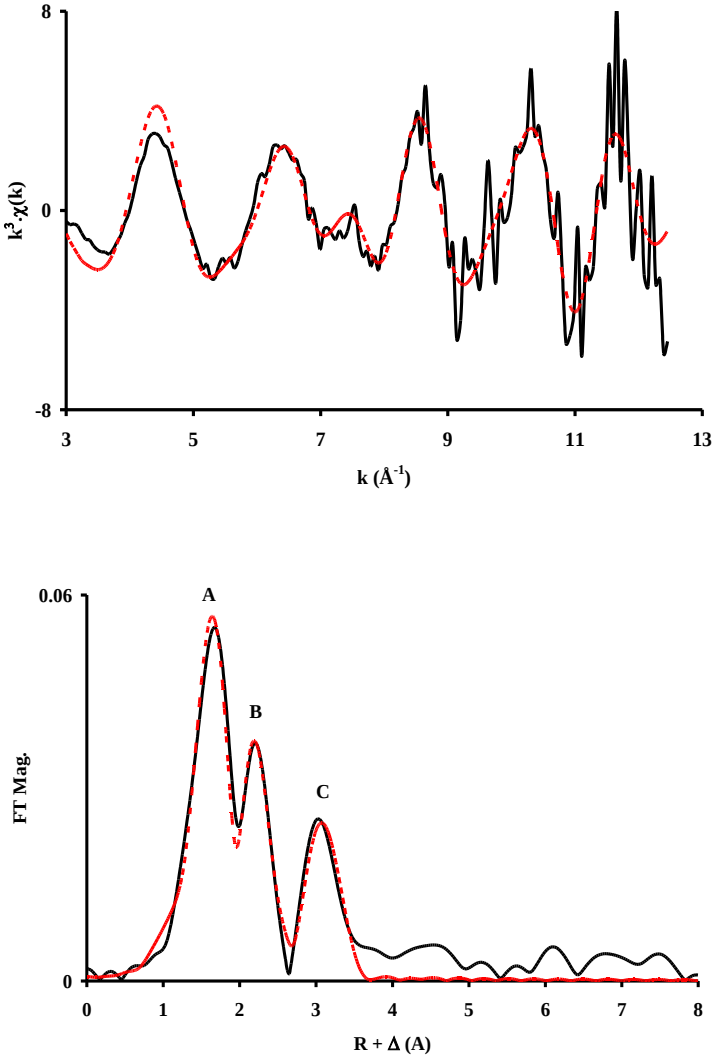

Figure 4. Fitted k^3-EXAFS spectra (top) and Fourier transform (bottom) of the k^3-EXAFS spectrum of Sample 1. Fit between k = 3 and 12.5 $Å^{-1}$. Experimental data in black and fit in red dots.

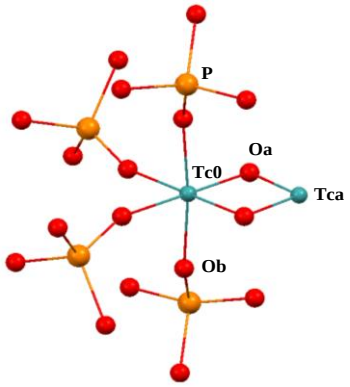

Figure 5. Ball and stick representation of the $\{Tc_2O_2(PO_4)_4\}$ fragment (a) used for the EXAFS analysis of Sample 1. Color of atom: Tc in blue; O in red and P in orange. Tc0 represents the absorbing atom.

Table 3. EXAFS fit parameters obtained by fit of the k^3-EXAFS spectra for Sample 1. ΔE_0 = 6.17 eV. Reduced-chi^2 = 78.8. R = 9.56%

Scattering Path	C.N	R (Å)	σ^2 (Å^2)
Tc0-Oa	0.5 ± 0.1	1.84(2)	0.003*
Tc0-Ob	4.3 ± 1.0	2.07(2)	0.006*
Tc0-Tca	0.7 ± 0.2	2.55(3)	0.003*
#Tc0-P (SS1)	5.0 ± 1.2 #	3.39(3)	0.006*
#Tc0-Ob-P (MS1)	10.0 ± 2.4 #	3.54(4)	0.012*

* Fixed parameter. # Correlated parameter.

The EXAFS results are consistent with the presence of a Tc(IV) atom in an octahedral environment coordinated to 5.0 ± 1.2 [DBP] units. As mentioned (*vide supra*) the [DBP] units could be coordinated as DBP^-, HDBP or $DBP.HDBP^-$. The Tc-P distance (3.39(3) Å) is shorter than the one in $[TcCl_4(TPPO)_2]$ (3.447 Å). This trend is also observed in U(VI) chemistry as the U-P distance in $[UO_2(TcO_4)_2(TPPO)_3]$ (avg. 3.730 Å)[43] is longer that the U-P distance in $[UO_2(DBP)_2]$ (3.621 Å) [44].

The presence of 0.7(2) Tc atom at 2.55(3) Å is consistent with the presence of the Tc_2O_2 unit. The Tc-Tc distance is ~0.2 Å longer than the one found by XRD in crystalline samples but comparable to the one found by EXAFS in amorphous or liquid samples for Tc(IV) species with a Tc_2O_2 unit (**Table 3**). Based on the EXAFS results and considering a neutral charge for extracted species [45], the formula $[Tc_2O_2(DBP)_4(HDBP)_4]$ (1) is proposed (**Figure 6**).

Table 4. Interatomic Tc-Tc and Tc-O(L) distances (Å) in Tc(IV) species with a Tc_2O_2 unit found by EXAFS (bold) and XRD.

Species	Tc-Tc	Tc-O(L)
$K_4T_2O_2(C_2O_4)_4.3H_2O$[16]	2.361(1)	2.020(1)-2.098(1)
$Tc_2O_2(H_2EDTA)_2.5H_2O$[34]	2.331(1)	2.004(4)-2.020(5)
Tc(IV) in 5 M CO_3^{2-}[46]	**2.51(3)**	**2.01(2)**
$Na_2[Tc_2O_2][NTA]_2.6H_2O$[41]	2.363(2)	2.034(3)-2.072(2)
Tc(IV) in 0.1M glyoxylate in 2M NaOH[32]	**2.582(4)**	**2.008(3)**
$[Tc_nO_y]^{4n-2y}$ in 0.1 M SO_4^{2-}[47]	**2.51(2)**	**2.04(2)**
Sample 1 (This work)	**2.55(3)**	**2.07(2)**

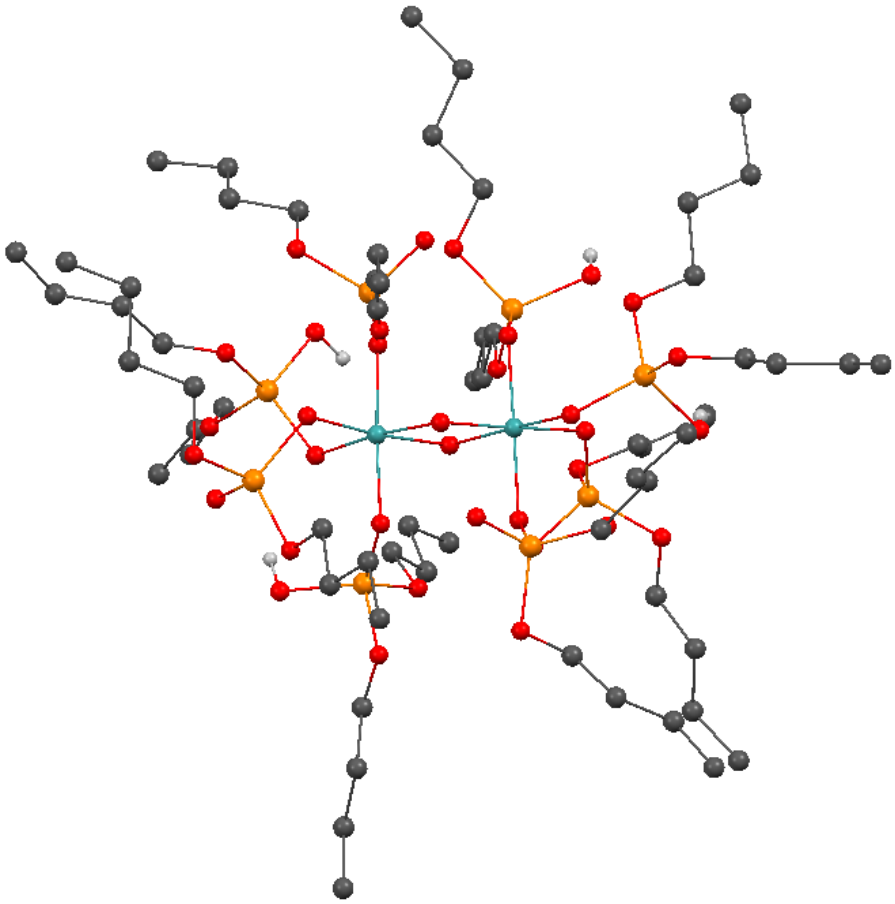

Figure 6. Ball and stick representation of the $[Tc_2O_2(DBP)_4(HDBP)_4]$ molecule. Color of atom: Tc in blue; O in red, C in dark grey, and P in orange. H atoms coordinated to C atoms are omitted for clarity. H atoms coordinated to O atoms are in light gray.

3.2 Sample 2

3.2.1 Study of reaction in Sample 2

The reaction between TcO_4^- and N_2H_4 in 3M HNO_3 ([Tc] = 0.005M, [N_2H_4] = 1M) was monitored for 48 hours by UV-Vis spectroscopy in Figure **7**. A blank sample of 3M HNO_3 was used as the background. Various concentrations of HNO_3 solutions were subjected to monitoring, with the 3M HNO_3 solution demonstrating the most favorable spectral characteristics, thereby serving as a representative proxy for 1M HNO_3. A clear solution is observed at the start of the reduction in **Figure 8**. After, an induction effect is seen after 2 hours, and the solution turns brown. The formation of the band at 400nm rises for the 24 hours. Following this, the signal doesn't fluctuate between 24 to 48 hours.

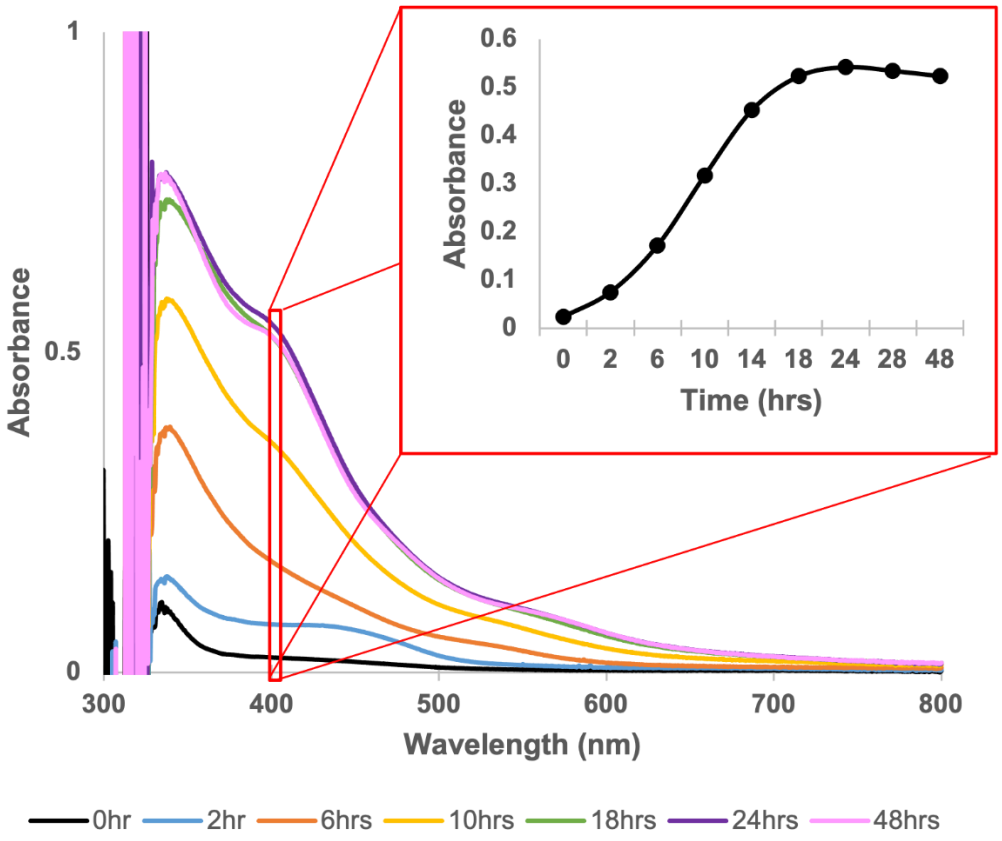

Figure 7. UV-Vis spectra and time dependence of the reduction of 0.005M Tc(VII) in 3M HNO_3 using 1M hydrazine over 48 hours.

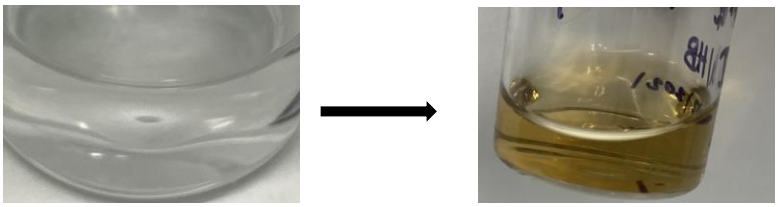

Figure 8. Reaction of TcO_4^- with N_2H_4 in 1M HNO_3 at t=0 hours (left) and t=48 hours (right).

3.2.2 EXAFS of Sample 2

The EXAFS spectrum of the Sample 2 was averaged, k^3-weighted and FT performed in the 3-12.5 $Å^{-1}$ k range. The FT (**Figure 9**) shows 3 peaks: Peak A at R + Δ ~ 1.62 Å, Peak B at ~ 2.25 Å and Peak C at ~ 3.06 Å. While the position of these peaks are similar to those in Sample 1, the FT magnitude of Peak B and C in both samples are significantly different which indicate that the species in Sample 1 and 2 to exhibit different structures. Attempts to fit the Fourier filtering on peak B using Tc0-Tca scattering path did not provide satisfactory results, which indicate that the species does not contain a Tc_2O_2 unit (**Figure S7 and Table S2**).

Peak B is due to the presence of N atoms from nitrate ligands and fit of the Fourier filtering considering Tc-N scattering path did provide satisfactory results (**Figure S8 and Table S3**). As the intensity and FWHM of Peak C in Sample 2 are larger than the one of Peak C in Sample 1, the presence of Tc atoms in the second coordination sphere was considered. In this hypothesis, the species in Sample 2 would consist of a linear Tc-O-Tc unit coordinated to [DBP] units and nitrate ligands. To investigate this hypothesis, the EXAFS spectrum was fit using the scattering path calculated in a putative $\{Tc_2O(PO_4)_3(NO_3)\}$ fragment (b) (**Figure 10**). The fragment (b) was constructed using the {Tc-O-P}, {Tc-O-Tc} and $\{Tc\text{-}NO_3\}$ metrics derived from $[TcCl_4(TPPO)_2]$, $[\{TcCl_3(DMSO)_2\}_2O]$[33] and $Cs[Zr(NO_3)_5]$[48] respectively.

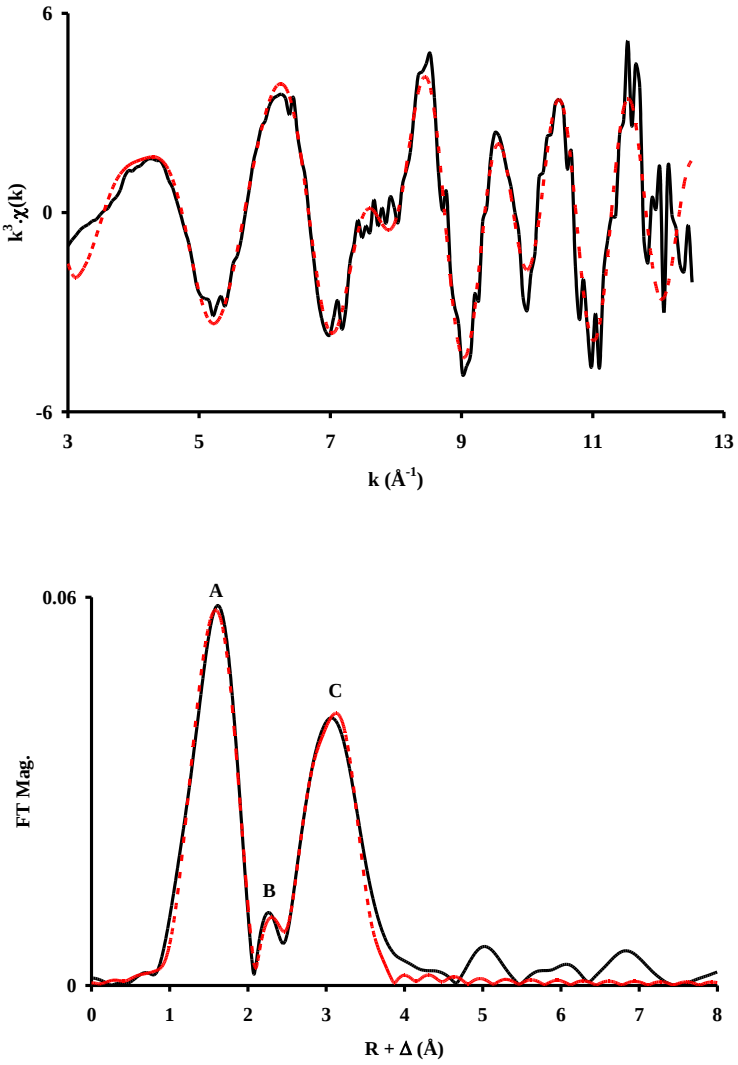

Figure 9. Fitted k^3-EXAFS spectra (top) and Fourier transform (bottom) of the k^3-EXAFS spectrum of Sample 2. Fit between k = 3 and 12.5 $Å^{-1}$. Experimental data in black and fit in red dots.

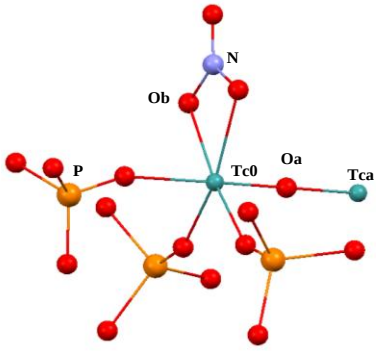

Figure 10. Ball and stick representation of the {$Tc_2O(PO_4)_3(NO_3)$} fragment (b) used for the EXAFS analysis of Sample 2. Color of atom: Tc in blue; O in red, N in purple and P in orange. Tc0 represents the absorbing atom.

For the fit, the Tc0-Oa, Tc0-Ob, and Tc0-P single scattering paths as well as the Tc0-Ob-P (MS1) and Tc0-Oa-Tca (MS2 and MS3) multi-scattering paths were used. The DWF values were fixed and the values of the C.N for the Tc0-Oa-Tca scattering paths were correlated (i.e., $C.N_{(MS2)} = 2.\ C.N_{(MS3)}$). The ΔE_0 was constrained to be the same value for each scattering path; all the other parameters were allowed to vary. The result of the fit (**Figure 9, Table 5**) indicates the environment of the absorbing atom to be comprised of 0.4(1) Oa atoms at 1.70(2) Å, 3.8 ± 1 Ob atoms at 2.11(2) Å, 0.7(2) N atoms at 2.70(3) Å, 2.8(7) P atoms at 3.36(3) Å and 0.7(2) Tc atoms at 3.57(4) Å.

Attempt to fit the EXAFS spectra of Sample 2 using only Tc0-Oa, Tc0-Ob, Tc0-P and Tc0-Ob-P (MS1) scattering paths in a similar manner to Sample 1 results in higher value of the reduced-chi^2 (297.01) which indicates that the model considering a Tc_2O unit

coordinated to DBP and nitrate ligands to be the most probable one (**Figure S9, Table S4**).

The presence of a Tc atom at 3.57(4) Å is consistent with the presence of the Tc_2O unit and comparable to the one found by EXAFS and XRD for Tc(IV) species with a Tc_2O unit (**Table 6**). The Tc-N distance is comparable to the one found for nitrate ligand coordinated to Zr(IV) in bidentate mode (2.707 - 2.763 Å). The Tc-P distance in Sample 2 (3.36(3) Å) is also comparable to the one in Sample 1 (3.39(3) Å) indicating the DBP possesses coordination mode in both samples. Based on the EXAFS results, the formula $[Tc_2O(NO_3)_2(DBP)_4(HDBP)_2]$ (2) is proposed (**Figure 11**). Similar to Sample 1, the presence of $[DBP.HDBP]^-$ dimers in (2) would lead to the formula $[Tc_2O(NO_3)_2(DBP)_2(DBP.HDBP)_2]$.

Table 5. EXAFS fit parameters obtained by fit of the k^3-EXAFS spectra for Sample 2. ΔE_0 = 4.28 eV. Reduced-chi^2: 9.5. R = 5.64 %

Scattering Path	C.N	R (Å)	σ^2 (Å^2)
Tc0-Oa (TcO_4^-)	0.4 ± 0.1	1.70(2)	0.001*
Tc0-Ob	3.8 ± 1.0	2.11(2)	0.005*
Tc0-N	0.7 ± 0.2	2.70(3)	0.003*
Tc0-P	2.8 ± 0.7	3.36(3)	0.002*
Tc0-P (MS1)	3.9 ± 1.0	3.44(3)	0.004*
#Tc0-Oa-Tca (MS2)	1.4 ± 0.4 #	3.57(4)#	0.004*
#Tc0-Oa-Tca (MS3)	0.7 ± 0.2 #	3.57(4)#	0.004*

* fixed parameters. #correlated parameter

Table 6. Interatomic Tc-Tc and Tc-O(L) distances (Å) in Tc(IV) species with a Tc_2O unit found by EXAFS (bold) and XRD.

Species	Tc-Tc	Tc-O(L)
$[Tc_2O(HSO_4)_4(H_2O)_2(OH)_2]$[49]	**3.62(4)**	**2.03(2)**
[$Tc_2OCl_{10}]^{4-}$[50]	**3.61(2)**	**/**
$[\{TcCl_3(CH_3CN)_2\}_2O]$[33]	3.5958(8)	/
$[\{TcCl_3(DMSO)_2\}_2O]$[33]	3.6269	2.06(1)-2.12(1)
$[Tc_2O(H_2O)_4Cl_6]$[35]	3.625(1)	2.116(4)-2.132(3)
Sample 2 (this work)	**3.58(4)**	**2.11(2)**

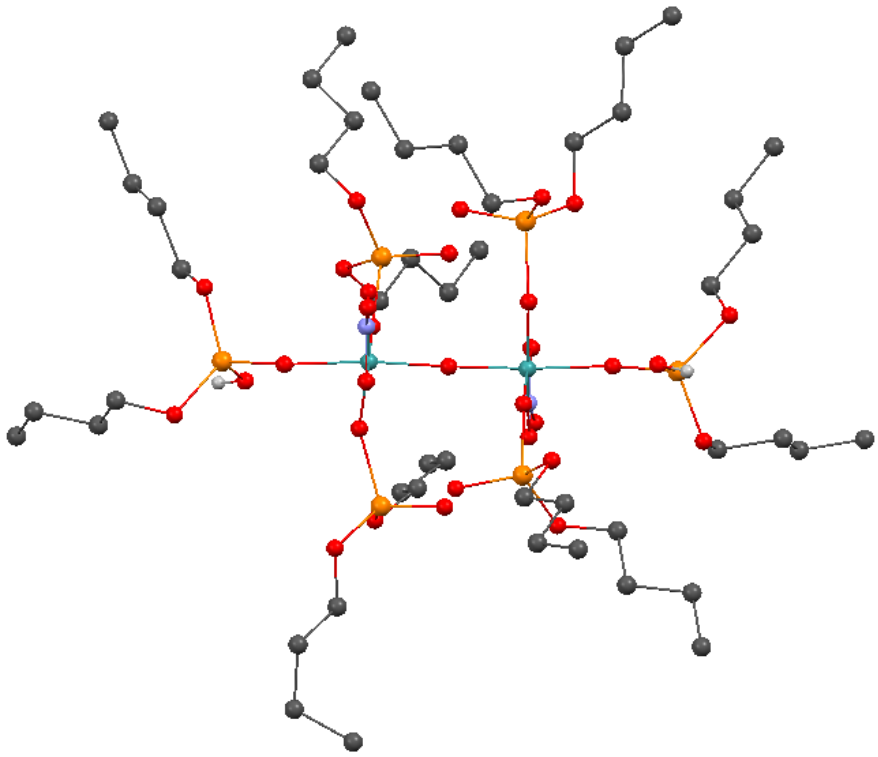

Figure 11. Ball and stick representation of the $[Tc_2O(NO_3)_2(DMP)_4(HDMP)_2]$ molecule. Color of atom: Tc in blue, O in red, C in grey, N in purple and P in orange. H atoms coordinated to C atoms are omitted for clarity. H atoms coordinated to O atoms are in light gray.

3.3 Sample 1 and Sample 2 interpretations

Results for Samples 1 and 2 show that Tc(IV) dimeric species with Tc_2O_2 and Tc_2O units, respectively, are formed in the extraction of Tc(IV) with HDBP from H_2O and 1 M HNO_3. The UV-visible spectra of sample 1 and 2 (Figure S2 and Figure S4) both exhibit

low energy bands (respectively at 499 nm and 510 nm) that are consistent with the presence of Tc(IV) dimeric species. Previous studies have shown that similar bands were observed in the spectra of Tc(IV) species with Tc_2O_2 unit (e.g., 503 nm in $K_4T_2O_2(C_2O_4)_4.3H_2O$)[16] and with Tc_2O unit (e.g., 505 nm for $[Tc_2O(HSO_4)_4(H_2O)_2(OH)_2]$[49]). It was proposed that for Tc(IV) dimeric species, low energy band at ~500 nm could be due to a □→□* transition[39]. This suggests that the formulation of extracted species is related to the nature of the Tc(IV) species in the aqueous phase (*vide supra*). For Sample 1, the Tc species in dodecane exhibits a similar core structure to that of the structural units in the $TcO_2{\cdot}xH_2O$ species in aqueous media. It has been proposed that the low-soluble $TcO_2{\cdot}xH_2O$ exhibits a zigzag chain structure consisting of edge-sharing $[TcO_6]$ octahedra [28]. In the zigzag chains of $TcO_2.xH_2O$, the Tc_2O_2 units with Tc-Tc distances (2.55 Å) same as to those in Sample 1 (2.55 Å) are observed. In our studies, the reaction of a $TcO_2.xH_2O$ aqueous suspension with HDBP results in the formation of a Tc(IV)-DBP solid (with a structure related to $TcO_2{\cdot}xH_2O$) that subsequently dissolve in dodecane. The dissolution of the Tc(IV)-DBP solid is accompanied by fragmentation of the chain-structure and during this fragmentation the Tc_2O_2 unit is preserved[51]. This mechanism is similar to the one proposed for the formation of Zr(IV)-DBP polymeric species after the extraction of $ZrOCl_2.8H_2O$ from 2M HNO_3 with HDBP/TBP/dodecane. It was postulated that a solid, $[Zr(HDBP)_2(NO_3)_2(OH)_2]$ with a chain-structure (Zr-Zr = ~3.1Å)[52,53] is initially formed upon extraction of Zr(IV) with HDBP. Following its formation, the $[Zr(HDBP)_2(NO_3)_2(OH)_2]$ solid undergoes a re-dissolution in the organic phase followed by dissociation of the chain into monomeric or polymeric species.

For Sample 2, results of our EXAFS spectroscopy indicate that a Tc(IV) species with the formula $[Tc_2O(NO_3)_x(H_2O)^{6-x}]$ is extracted with HDBP as $[Tc_2O(NO_3)_2(DBP)_4(HDBP)_2]$ or $[Tc_2O(NO_3)_2(DBP)_2(DBP.HDBP)_2]$. In this domain of acidity, the Tc(IV) speciation in HNO_3 would be comparable to the one in chloride media which indicates the species with Tc_2O unit to be dominant in the pH domain 0.25-1[43]. Previous studies have shown that polymeric species could be extracted from nitrate aqueous media with TBP and preserve their polynuclear nature in the organic media (**Table 8**). It has been shown that following extraction polymeric species could either 1) aggregate to form higher nuclearity complexes (i.e., Ce(IV)), 2) conserve their nuclearity (Th(IV), Hf(IV)) or 3) extract as colloidal species in the form of Pu(IV). Furthermore it has been shown that a Ru polymeric species with a Ru_2O_2 unit is present in dodecane after extraction of Ru(III) complexes with TBP from 1 M HNO_3[54].

Table 7. Nature of species after extraction of M(IV) (M= Ce, Hf, Th, Pu) species with TBP from nitrate media.

Species in aqueous	Aqueous media	Organic media	Extracted species
Ce(IV) dimers with $[Ce\text{-}O\text{-}Ce]^{6+}$ unit	3 M HNO_3	dodecane/TBP	$Ce_4O_4.xNO_3.yTBP$ [55]
$[Hf_4(OH)_8.16H_2O]^{8+}$	7 M $LiNO_3$	TBP	$Hf_n(OH)_{2n}(NO_3)_{2n}.nTBP$ (n=2,3,4)
$[Th_4(OH)_{10}(NO_3)_x]^{6-x}$	7 M $LiNO_3$	TBP	$[Th_4(OH)_{10}(NO_3)_6].4TBP$
Pu(IV)-colloid	0.1 M HNO_3	TBP/dodecane	Pu(IV)-TBP colloid[56]

Chapter 4: Conclusion and Future Work

For the first time, the speciation of Tc after extraction of Tc(IV) from aqueous media (H_2O and 1 M HNO_3) by an alkylphosphate (i.e., HDBP) in n-dodecane has been investigated by XAFS spectroscopy. XAFS results show the formation of dimeric species with Tc_2O_2 and Tc_2O units and the proposed formulae for extracted species are $[Tc_2O_2(DBP)_4(HDBP)_4]$ or $[Tc_2O_2(DBP{\cdot}HDBP)_4]$ in the absence of nitrate and $[Tc_2O(NO_3)_2(DBP)_4(HDBP)_2]$ or $[Tc_2O(NO_3)_2(DBP)_2(DBP{\cdot}HDBP)_2]$) in the presence of nitrates. The interatomic Tc-Tc distances found in these units are similar to those found in well-known Tc(IV) dinuclear species. The new structural data, first reported here, include the Tc-N and Tc-P distances for a nitrate and alkyl phosphate ligands coordinated to a Tc atom.

The study shows that the speciation of Tc in the organic phase is closely related to its speciation in the aqueous extraction phase. For Sample 1, the extracted species exhibits a similar core structure to the species in water ($TcO_2.xH_2O$). The study of Sample 2 provides also insight into the speciation of Tc(IV) in nitric acid, and $[Tc_2O(NO_3)_x(H_2O)^{6-x}]$ is proposed to be the dominant species in 1 M HNO_3. These results confirm the importance of the preparation methods of the Tc(IV) aqueous solution prior to extraction and how much they influence the Tc speciation in the organic extraction media. These observations outline the complexity of Tc separation chemistry and provide insight into behavior of Tc during the reprocessing of UNF. Any deviation during UNF processing that affect the reduction conditions of Tc(VII) (e.g., acidity) could potentially lead to the formation of either Tc dimeric species or monomeric nitrate species in the various streams. In order to predict Tc behavior, the consideration of such

Tc(IV) species in simulation scenario should be considered. First of all, the spectroscopic studies of Tc speciation in organic phases after extraction from HNO_3 > 3M would aim for a better understanding of the Tc behavior in the UNF reprocessing matrices. The structural data and semi-optimized model provided here provide support for such work.

Appendix

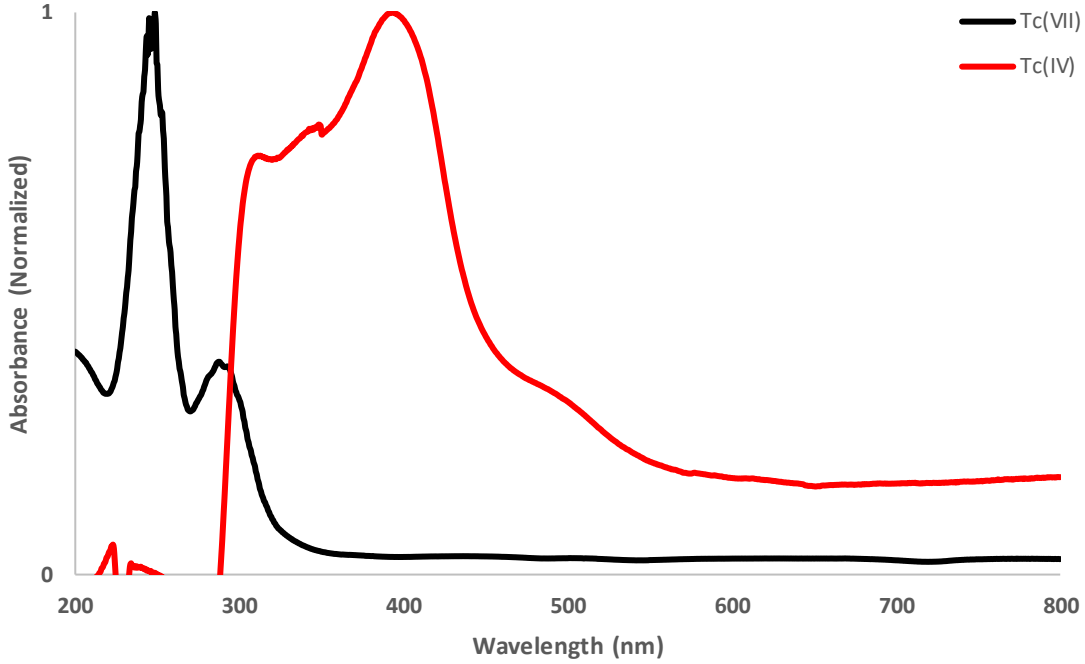

Figure S1. UV-Vis spectra of KTcO4 (Tc(VII)) in water and aliquot of hydrazine reduced Tc in HNO_3 in concentrated HCl.

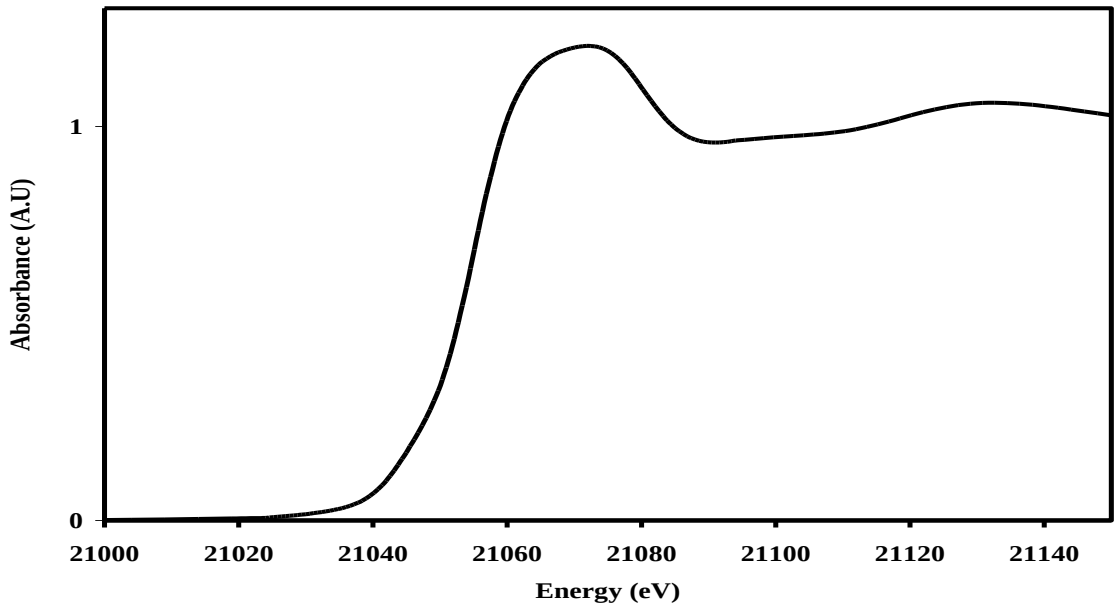

Figure S2. Normalized XANES spectra of Sample 1.

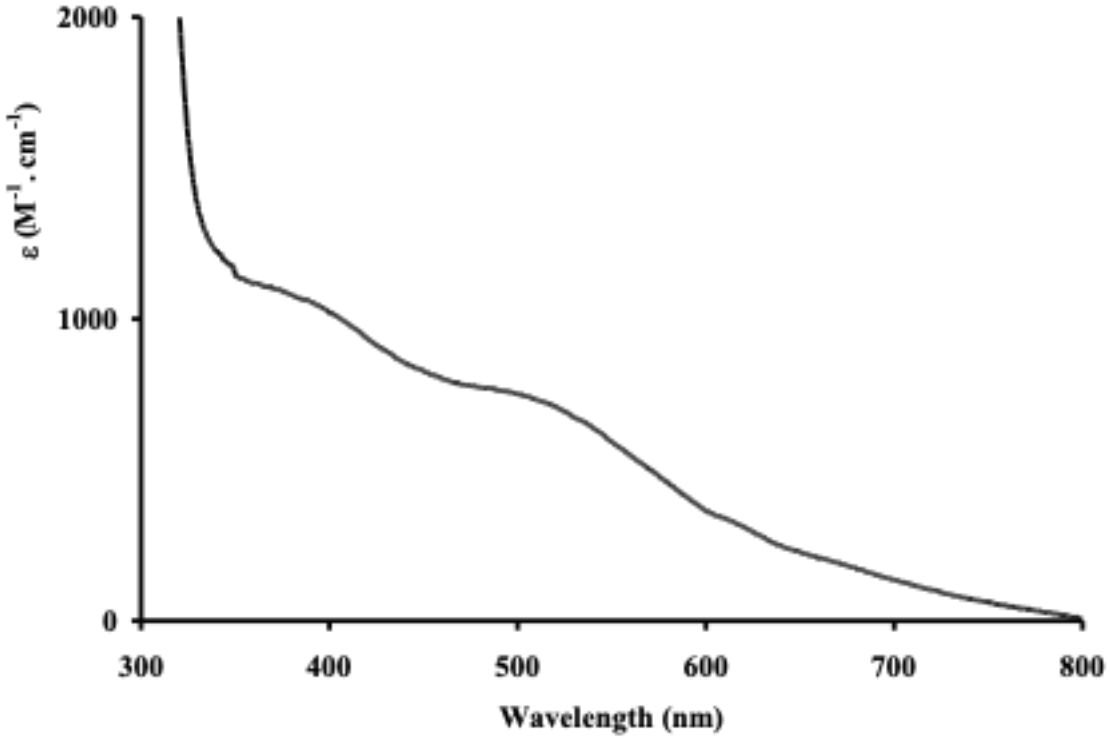

Figure S3. UV-Visible spectra of Sample 1 after dilution 1:50 using HDBP-in dodecane.

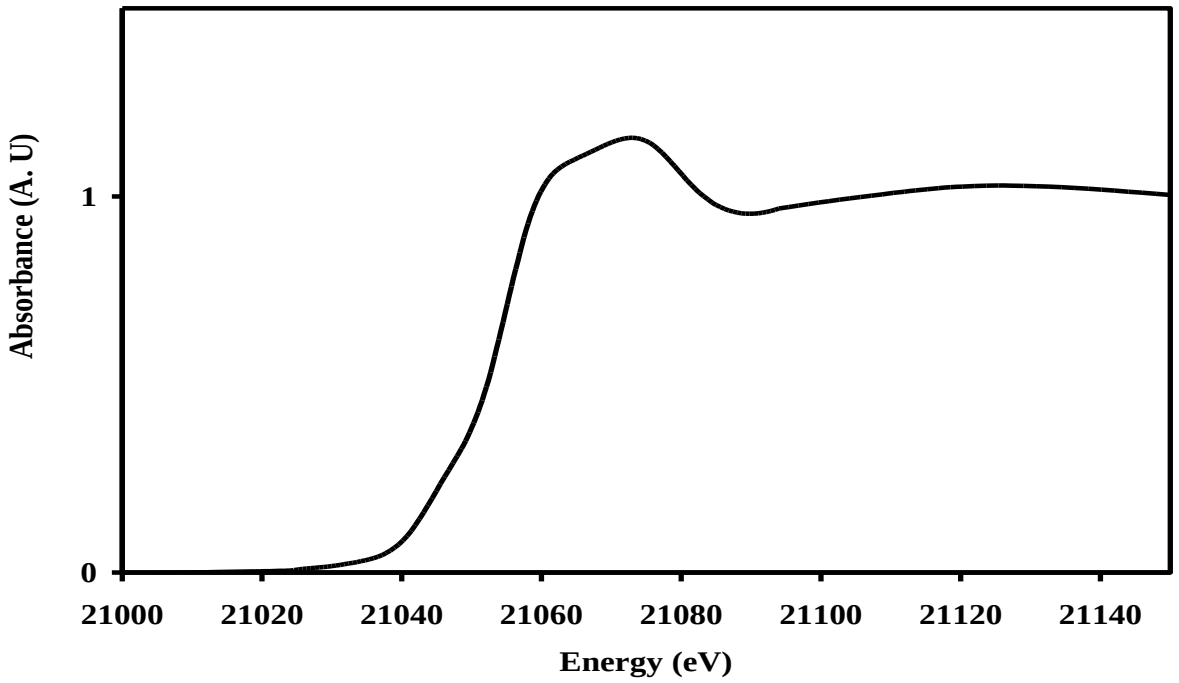

Figure S4. Normalized XANES spectra of Sample 2.

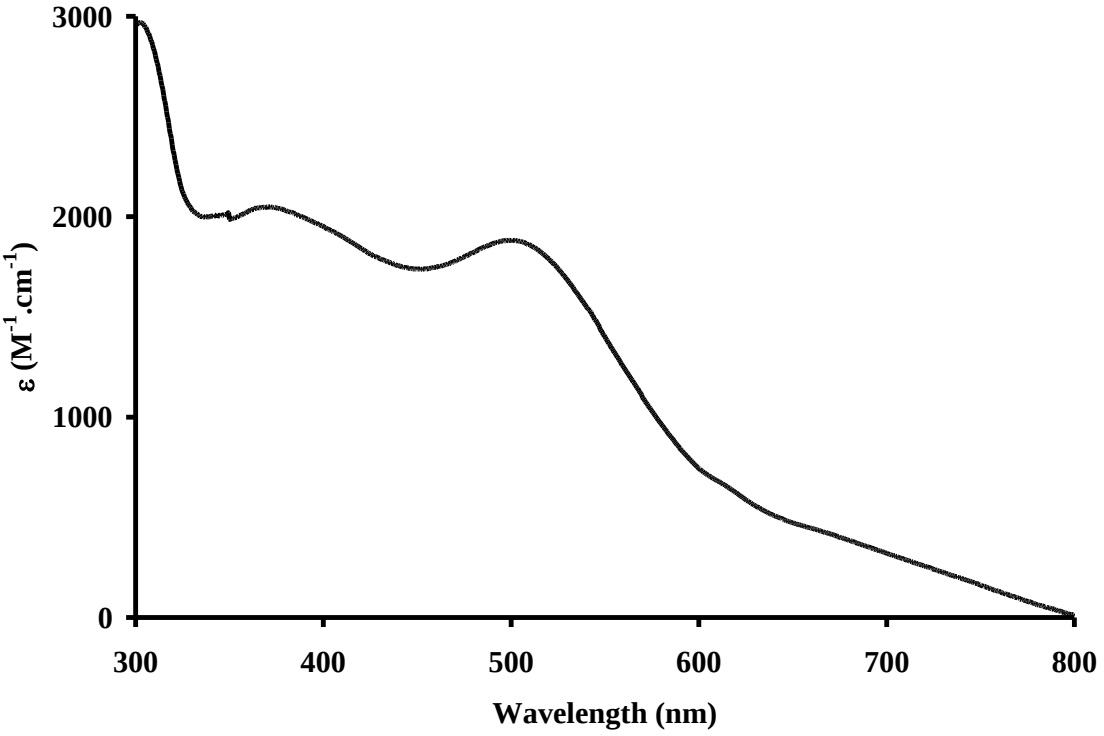

Figure S5. UV-Visible spectra of Sample 2 after dilution 1:50 using HDBP-in dodecane.

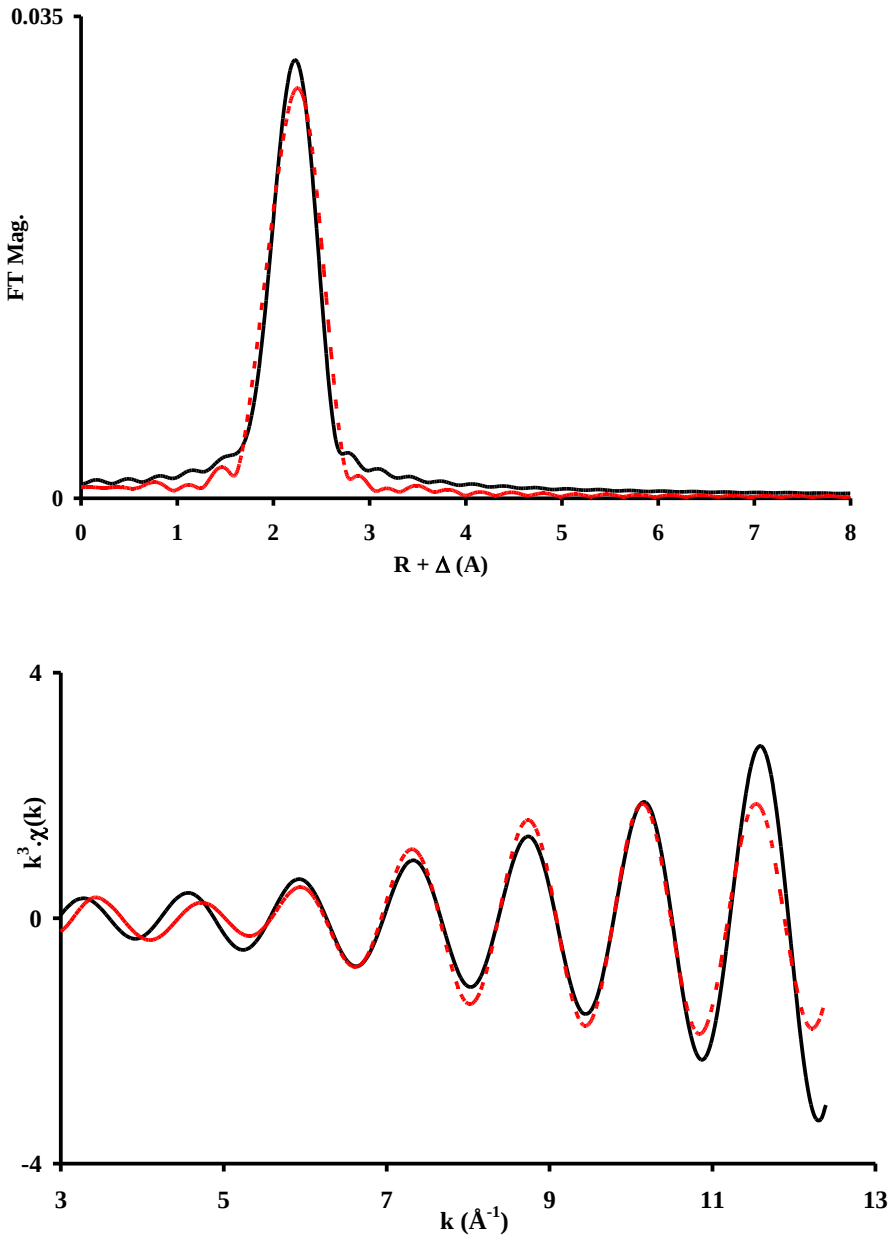

Figure S6. Adjustment of filtered Fourier transform and back transformed k^3-EXAFS spectra of the Sample 1 considering Tc0-Tc scattering. Fourier Filtering between R+ □ = 1.65 and 2.45 Å ; adjustment between k = 3 and 12.5 $Å^{-1}$. Experimental data in black and fit in red dots.

Table S1. EXAFS fit parameters obtained by adjustment of filtered Fourier transform and back transformed k3-EXAFS spectra of the Sample 1. Fourier Filtering between R+ □ = 1.65 and 2.45 Å. ΔE_0 =12.40 eV. Reduced-chi^2 = 0.9

Scattering	C.N	R (Å)	□^{2} (Å^2)
Tc0-Tc	0.7	2.57	0.003*

* fixed parameters. #correlated parameter

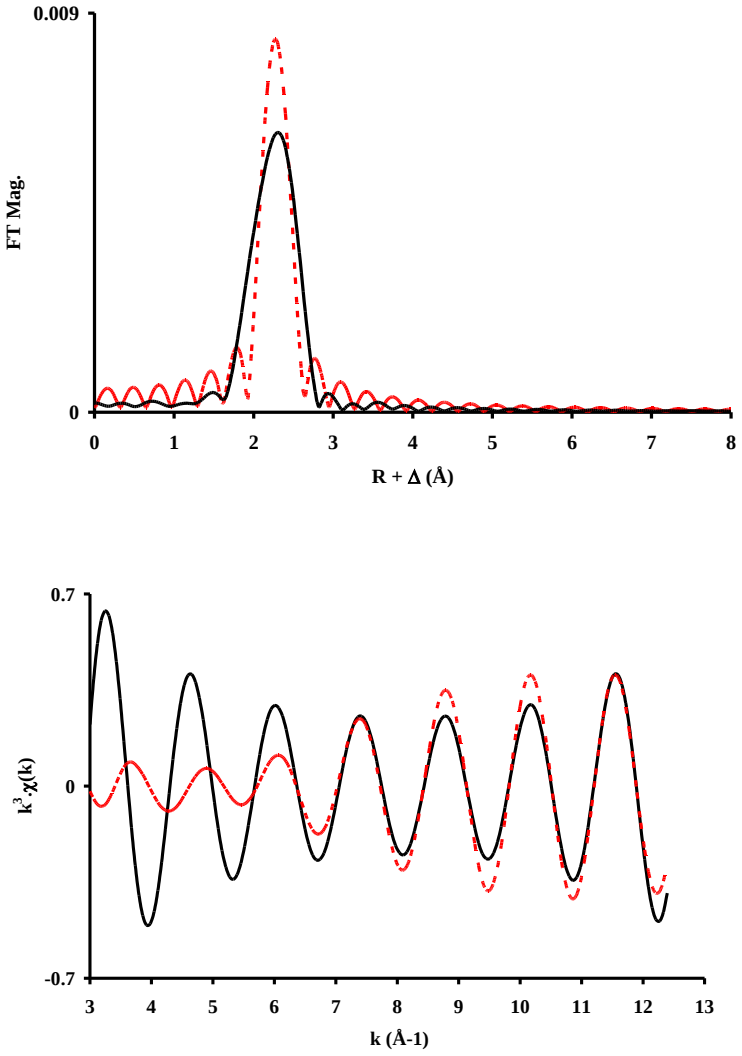

Figure S7. Adjustment of filtered Fourier transform and back transformed k^3-EXAFS spectra of the Sample 2 considering Tc0-Tc scattering. Fourier Filtering between R+ □ = 2.05 and 2.45 Å. adjustment between k = 3 and 12.5 $Å^{-1}$. Experimental data in black and fit in red dots.

Table S2. EXAFS fit parameters obtained by adjustment of filtered Fourier transform and back transformed k^3-EXAFS spectra of the Sample 1. Fourier Filtering between R+ □ = 2.05 and 2.45 Å ; ΔE_0 =18.34 eV. Reduced-chi^2 = 2068.55

Scattering	C.N	R (Å)	□^{2} (Å^2)
Tc0-Tc	0.1	2.59	0.003*

* fixed parameters.

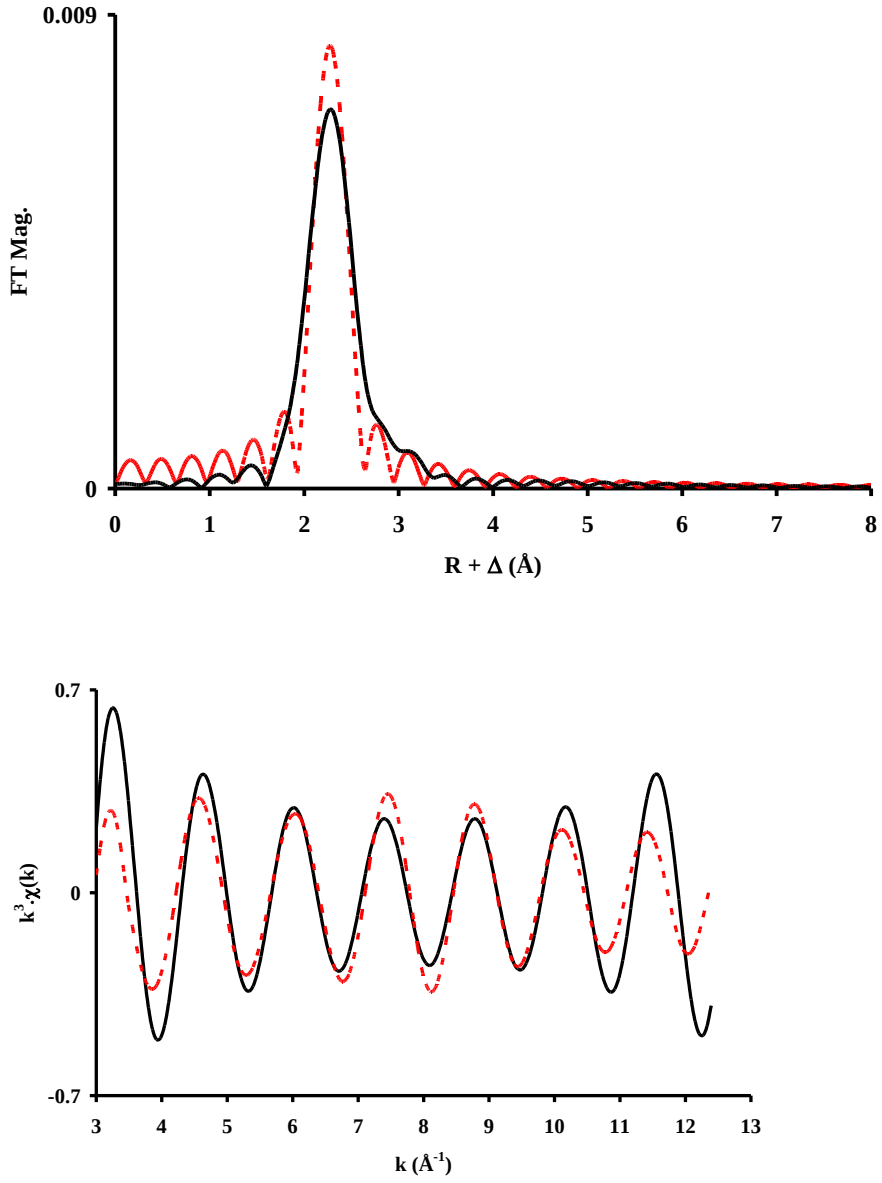

Figure S8. Adjustment of filtered Fourier transform and back transformed k^3-EXAFS spectra of the Sample 2 considering Tc0-N scattering. Fourier Filtering between R+ □ = 2.05 and 2.45 Å. adjustment between k = 3 and 12.5 $Å^{-1}$. Experimental data in black and fit in red dots.

Table S3. EXAFS fit parameters obtained by adjustment of filtered Fourier transform and back transformed k^3-EXAFS spectra of the Sample 2 considering Tc0-N scattering. Fourier Filtering between R+ □ = 2.05 and 2.45 Å. ΔE_0 = 11.37 eV. Reduced-chi^2 = 604.18

Scattering	C.N	R (Å)	□^{2} (Å^2)
Tc0-N	0.9	2.76	0.003*

* fixed parameters.

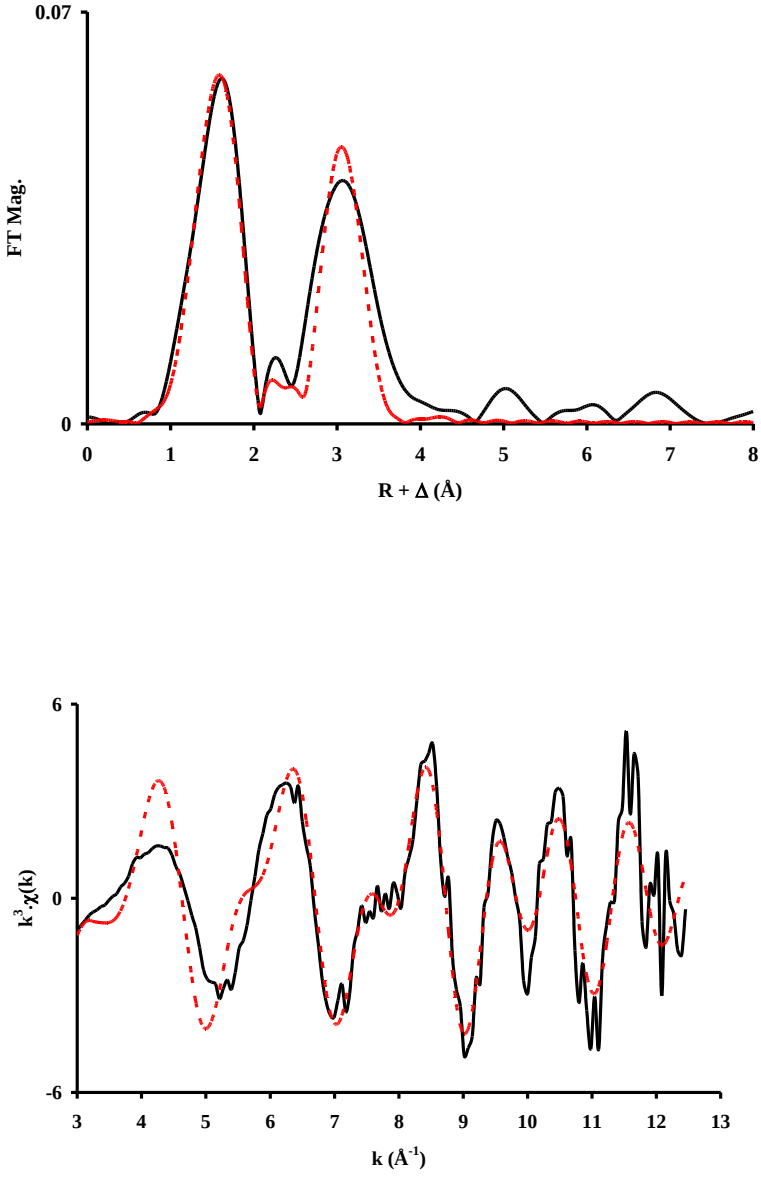

Figure S9. Fitted k^3-EXAFS spectra (top) and Fourier transform (bottom) of the k^3-EXAFS spectrum of Sample 2 considering Tc-O and Tc-P scattering. Adjustment between k = 3 and 12.5 $Å^{-1}$. Experimental data in black and fit in red dots.

Table S4. EXAFS fit parameters obtained by adjustment of the k^3-EXAFS spectra for Sample 2. ΔE_0 = 4.56 eV. Reduced-chi^2 =297.01

Scattering	C.N	R (Å)	□^{2} (Å^2)
Tc0-Oa	0.4	1.70	0.003*
Tc0-Ob	4.3	2.11	0.005*
Tc0-P #	11.2	3.38	0.006*
Tc0-OP (MS1)#	22.4	3.52	0.012*

* fixed parameters. #correlated parameter

Bibliography

(1) Johnstone, E. V.; Yates, M. A.; Poineau, F.; Sattelberger, A. P.; Czerwinski, K. R. Technetium: The First Radioelement on the Periodic Table. *J Chem Educ* **2017**, *94* (3), 320–326. https://doi.org/10.1021/acs.jchemed.6b00343.

(2) Lumetta, G. J.; Allred, J. R.; Bryan, S. A.; Hall, G. B.; Levitskaia, T. G.; Lines, A. M.; Sinkov, S. I. Simulant Testing of a Co-Decontamination (CoDCon) Flowsheet for a Product with a Controlled Uranium-to-Plutonium Ratio. *Separation Science and Technology (Philadelphia)* **2019**, *54* (12), 1977–1984. https://doi.org/10.1080/01496395.2019.1594899.

(3) Lovasic, Z. Spent Fuel Reprocessing Options. *Nuclear Fuel Cycle and Materials Section* **2008**, No. August, 151.

(4) George, K.; Masters, A. J.; Livens, F. R.; Sarsfield, M. J.; Taylor, R. J.; Sharrad, C. A. A Review of Technetium and Zirconium Extraction into Tributyl Phosphate in the PUREX Process. *Hydrometallurgy* **2022**, *211* (April), 105892. https://doi.org/10.1016/j.hydromet.2022.105892.

(5) Mincher, B. J.; Modolo, G.; Mezyk, S. P. Review Article: The Effects of Radiation Chemistry on Solvent Extraction: 1. Conditions in Acidic Solution and a Review of TBP Radiolysis. *Solvent Extraction and Ion Exchange* **2009**, *27* (1), 1–25. https://doi.org/10.1080/07366290802544767.

(6) Wright, A.; Paviet-Hartmann, P. Review of Physical and Chemical Properties of Tributyl Phosphate/Diluent/Nitric Acid Systems. *Sep Sci Technol* **2010**, *45* (12), 1753–1762. https://doi.org/10.1080/01496395.2010.494087.

(7) Braatz, A. D.; Antonio, M. R.; Nilsson, M. Structural Study of Complexes Formed by Acidic and Neutral Organophosphorus Reagents. *Dalton Transactions* **2017**, *46* (4), 1194–1206. https://doi.org/10.1039/c6dt04305d.

(8) Henry, H. E.; Jenkins, W. J. Uranium(IV) Nitrate as Areducing Agent for Plutonium(IV) in the PUREX Process. *Dp-808* **1965**.

(9) Harlow, D. G.; Felt, R. e.; Agnew, S.; Barney, S.; McKibben, J. M.; Garber, R.; Lewis, M. Technical Report on Hydroxylamine Nitrate. *U.S. Department Of Energy* **1998**, No. February, 19.

(10) Kumar, S.; Koganti, S. B. Next-Generation Purex Flowsheets with Acetohydroxamic Acid as Complexant for FBR and Thermal-Fuel Reprocessing. *Solvent Extr.: Fundam. Ind. Appl., Proc. ISEC 2008 Int. Solvent Extr. Conf.* **2008**, *1* (September 2008), 635–640. https://doi.org/10.13140/2.1.3706.4007.

(11) Goletskii, N. D.; Zilberman, B. Y.; Fedorov, Y. S.; Kudinov, A. S.; Timoshuk, A. A.; Sytnik, L. V.; Puzikov, E. A.; Rodionov, S. A.; Krinitsyn, A. P.; Ryazantsev, V. I.; Ryabkov, D. V. Ways of Technetium and Neptunium Localization in Extraction Reprocessing of Spent Nuclear Fuel from Nuclear Power Plants. *Radiochemistry* **2014**, *56* (5), 501–514. https://doi.org/10.1134/S1066362214050099.

(12) Melent'ev, A. B.; Mashkin, A. N.; Tugarina, O. V.; Kolupaev, D. N.; German, K. E.; Tananaev, I. G. Effect of Complexing Agents (DTPA and Oxalic Acid) on the Extraction Behavior of Technetium in

the TBP-N2H5NO 3-HNO3 System. *Radiochemistry* **2011**, *53* (2), 172–177. https://doi.org/10.1134/S106636221102010X.

(13) Chotkowski, M. Extraction of Moderate Oxidation State Technetium Species between 30 % Tri-n-Butyl Phosphate and H2SO4/HNO3. *J Radioanal Nucl Chem* **2016**, *307* (1), 457–462. https://doi.org/10.1007/s10967-015-4122-5.

(14) Garraway, J.; Wilson, P. D. The Technetium-Catalysed Oxidation of Hydrazine by Nitric Acid. *Journal of The Less-Common Metals* **1984**, *97* (C), 191–203. https://doi.org/10.1016/0022-5088(84)90023-7.

(15) Boukis, N.; Kanellakopulos, B. K. The Interaction of Tetravalent Technetium with Dibutyl Phosphoric Acid. *Radiochim Acta* **1990**, *49* (3), 141–146. https://doi.org/10.1524/ract.1990.49.3.141.

(16) Alberto, R.; Anderegg, G.; Albinati, A. Synthesis and X-Ray Structure of a New Tc(IV) Oxalato Complex: K4[(C2O4)2Tc(μ-O)2Tc(C2O4)2]·3H2O. *Inorganica Chim Acta* **1990**, *178* (1), 125–130. https://doi.org/10.1016/S0020-1693(00)88144-X.

(17) Poineau, F.; Sattelberger, A. P.; Lu, E.; Liddle, S. T. Group 7 Metal-Metal Bonds. *Molecular Metal-Metal Bonds: Compounds, Synthesis, Properties* **2015**, No. Ii, 175–224. https://doi.org/10.1002/9783527673353.ch7.

(18) Motokawa, R.; Kobayashi, T.; Endo, H.; Mu, J.; Williams, C. D.; Masters, A. J.; Antonio, M. R.; Heller, W. T.; Nagao, M. A Telescoping View of Solute Architectures in a Complex Fluid System. *ACS Cent Sci* **2019**, *5* (1), 85–96. https://doi.org/10.1021/acscentsci.8b00669.

(19) Tkac, P.; Momen, M. A.; Breshears, A. T.; Brown, M. A.; Vandegrift, G. F. Molybdenum(VI) Coordination in Tributyl Phosphate Chloride Based System. *Ind Eng Chem Res* **2018**, *57* (16), 5661–5669. https://doi.org/10.1021/acs.iecr.8b00590.

(20) Dirks, T.; Dumas, T.; Solari, P. L.; Charbonnel, M. C. Ruthenium Nitrosyl Structure in Solvent Extraction Systems: A Comparison of Tributyl Phosphate, Tetrabutyl Urea, N-Methyl, N-Octyl Ethylhexanamide, and N, N, N', N'-Tetraoctyl Diglycolamide. *Ind Eng Chem Res* **2019**, *58* (32), 14938–14946. https://doi.org/10.1021/acs.iecr.9b02555.

(21) Alberti, G.; Costantino, U.; Allulli, S.; Tomassini, N. Crystalline Zr(R-PO3)2 and Zr(R-OPO3)2 Compounds (R = Organic Radical). A New Class of Materials Having Layered Structure of the Zirconium Phosphate Type. *Journal of Inorganic and Nuclear Chemistry* **1978**, *40* (6), 1113–1117. https://doi.org/10.1016/0022-1902(78)80520-X.

(22) Maya, L. Structure and Chromatographic Applications of Crystalline Zr(OPO3R)2; R = Butyl, Lauryl and Octylphenyl. *Inorganic and Nuclear Chemistry Letters* **1979**, *15* (5–6), 207–212. https://doi.org/10.1016/0020-1650(79)80130-0.

(23) Lanari, D.; Montanari, F.; Marmottini, F.; Piermatti, O.; Orr, M.; Vaccaro, L. New Zirconium Hydrogen Phosphate Alkyl and/or Aryl Phosphonates with High Surface Area as Heterogeneous Brønsted Acid Catalysts for Aza-Diels-Alder Reaction in Aqueous Medium. *J Catal* **2011**, *277* (1), 80–87. https://doi.org/10.1016/j.jcat.2010.10.012.

(24) Boyd, G. E. Promethium and Technetium. *J. Chem. Educ.* **1959**, *36* (1), 3–14.

(25) Davison, A.; Trop, H. S.; Depamphilis, B. V. Tetrabutylammonium Tetrachlorooxo- Technetate(v). No. V, 160–162.

(26) Anderson, T. L.; Braatz, A.; Ellis, R. J.; Antonio, M. R.; Nilsson, M. Synergistic Extraction of Dysprosium and Aggregate Formation in Solvent Extraction Systems Combining TBP and HDBP. *Solvent Extraction and Ion Exchange* **2013**, *31* (6), 617–633. https://doi.org/10.1080/07366299.2013.787023.

(27) Meyer, R. E.; Arnold, W. D.; Case, F. I. Valence Effects on Solubility and Sorption: The Solubility of Tc(IV) Oxides, Report No. NUREG/CR-4309. **1986**.

(28) Poineau, F.; Weck, P. F.; Burton-Pye, B. P.; Denden, I.; Kim, E.; Kerlin, W.; German, K. E.; Fattahi, M.; Francesconi, L. C.; Sattelberger, A. P.; Czerwinski, K. R. Reactivity of HTcO4 with Methanol in Sulfuric Acid: Tc-Sulfate Complexes Revealed by XAFS Spectroscopy and First Principles Calculations. *Dalton Transactions* **2013**, *42* (13), 4348–4352. https://doi.org/10.1039/c3dt32951h.

(29) Spitsyn V.I., Kryuchkov S.V., and K. A. F. Reduction of Pertechnetate Ions in Nitric Acid via Hydrazine.Pdf. 1983, pp 471–476.

(30) Grate, J. W.; O'Hara, M. J.; Egorov, O. B. *Automated Radiochemical Separation, Analysis, and Sensing*; Elsevier Inc., 2020; Vol. 2. https://doi.org/10.1016/B978-0-12-814395-7.00011-8.

(31) Ravel, B.; Newville, M. ATHENA, ARTEMIS, HEPHAESTUS: Data Analysis for X-Ray Absorption Spectroscopy Using IFEFFIT. *J Synchrotron Radiat* **2005**, *12* (4), 537–541. https://doi.org/10.1107/S0909049505012719.

(32) Ressler, T. WinXAS: A Program for X-Ray Absorption Spectroscopy Data Analysis under MS-Windows. *J Synchrotron Radiat* **1998**, *5* (2), 118–122. https://doi.org/10.1107/S0909049597019298.

(33) Rehr, J. J.; Albers, R. C. Theoretical Approaches to X-Ray Absorption Fine Structure. *Rev Mod Phys* **2000**, *72* (3), 621–654. https://doi.org/10.1103/RevModPhys.72.621.

(34) Ravel, B. Data Analysis : Crystallography the X-Ray Absorption Spectroscopist ATOMS : Crystallography for the X-Ray. *Synchrotron, J Spectroscopist, Absorption* **2001**, No. 2000, 2000–2002.

(35) Penner-Hahn, J. E. Characterization of "Spectroscopically Quiet" Metals in Biology. *Coord Chem Rev* **2005**, *249* (1–2), 161–177. https://doi.org/10.1016/j.ccr.2004.03.011.

(36) Hanwell, M.D., Curtis D.E., Lonie, D.C., Vandermeersch T., Zurek, E., H. G. R. Avogadro: An Advanced Semantic Chemical Editor, Visualization, and Analysis Platform. *Adv Math (N Y)* **2014**, *262*, 476–483. https://doi.org/10.1016/j.aim.2014.05.019.

(37) Oliveira, A. F.; Kuc, A.; Heine, T.; Abram, U.; Scheinost, A. C. Shedding Light on the Enigmatic TcO2 · XH2O Structure with Density Functional Theory and EXAFS Spectroscopy**. *Chemistry - A European Journal* **2022**, *28* (59). https://doi.org/10.1002/chem.202202235.

(38) Rodriguez, E. E.; Poineau, F.; Llobet, A.; Sattelberger, A. P.; Bhattacharjee, J.; Waghmare, U. V.; Hartmann, T.; Cheetham, A. K. Structural Studies of TcO2 by Neutron Powder Diffraction and First-Principles Calculations. *J Am Chem Soc* **2007**, *129* (33), 10244–10248. https://doi.org/10.1021/ja0727363.

(39) Lukens, W. W.; Bucher, J. J.; Edelstein, N. M.; Shuh, D. K. Products of Pertechnetate Radiolysis in Highly Alkaline Solution: Structure of TcO2·xH2O. *Environ Sci Technol* **2002**, *36* (5), 1124–1129. https://doi.org/10.1021/es015653+.

(40) Hagenbach, A.; Yegen, E.; Abram, U. Technetium Tetrachloride as A Precursor for Small Technetium(IV) Complexes. *Inorg Chem* **2006**, *45* (18), 7331–7338. https://doi.org/10.1021/ic060896u.

(41) Anderegg, G.; Miiller, E.; Zollinger, K.; Hans-Beat, B. Preparation, Characterization, Crystal and Molecular Structure of Na2 [N (CH2C00),Tc (IV) (JPO),~TC (1V)N (CH2C00),] . 6 H 2 0. **1983**, *66* (152), 1593–1598.

(42) Servaes, K., Hennig, C., Gorller-Walrand, C. *EXAFS AND UV-VIS INVESTIGATION OF THE FIRST CO-ORDINATION SPHERE OF THE URANYL ION IN UO2(NO3)2(TBP)*; 2007; Vol. NEA No. 62.

(43) Sarsfield, M. J.; Sutton, A. D.; May, I.; John, G. H.; Sharrad, C.; Helliwell, M. Coordination of Pertechnetate [TcO4]- to Actinides. *Chemical Communications* **2004**, *765* (20), 2320–2321. https://doi.org/10.1039/b404424j.

(44) Burns, J. H. Solvent-Extraction Complexes of the Uranyl Ion. **1983**, No. 8, 1174–1178.

(45) Wilson, A. M.; Bailey, P. J.; Tasker, P. A.; Turkington, J. R.; Grant, R. A.; Love, J. B. Solvent Extraction: The Coordination Chemistry behind Extractive Metallurgy. *Chem Soc Rev* **2014**, *43* (1), 123–134. https://doi.org/10.1039/c3cs60275c.

(46) Ghalei, M.; Vandenborre, J.; Poineau, F.; Blain, G.; Solari, P. L.; Rôques, J.; Haddad, F.; Fattahi, M. Speciation of Technetium in Carbonate Media under Helium Ions and γ Radiation. *Radiochim Acta* **2019**, *107* (2), 105–113. https://doi.org/10.1515/ract-2018-2939.

(47) Vichot, L.; Ouvrard, G.; Montavon, G.; Fattahi, M.; Musikas, C.; Grambow, B. XAS Study of Technetium(IV) Polymer Formation in Mixed Sulphate/Chloride Media. *Radiochim Acta* **2002**, *90* (9–11), 575–579. https://doi.org/10.1524/ract.2002.90.9-11_2002.575.

(48) Morozov, I. V.; Fedorova, A. A.; Palamarchuk, D. V.; Troyanov, S. I. Synthesis and Crystal Structures of Zirconium (IV) Nitrate Complexes. *Russian Chemical Bulletin,INternational Edition* **2005**, *54* (1), 93–98.

(49) Ferrier, M.; Roques, J.; Poineau, F.; Sattelberger, A. P.; Unger, J.; Czerwinski, A. K. R. Speciation of Technetium in Sulfuric Acid/Hydrogen Sulfide Solutions. *Eur J Inorg Chem* **2014**, No. 12, 2046–2052. https://doi.org/10.1002/ejic.201301410.

(50) Poineau, F.; Fattahi, M.; Montavon, G.; Grambow, B. Condensation Mechanisms of Tetravalent Technetium in Chloride Media. *Radiochim Acta* **2006**, *94* (5), 291–299. https://doi.org/10.1524/ract.2006.94.5.291.

(51) Richter, J.; Ruck, M. Synthesis and Dissolution of Metal Oxides in Ionic Liquids and Deep Eutectic Solvents. *Molecules* **2020**, *25* (1). https://doi.org/10.3390/molecules25010078.

(52) Miyake, C.; Hirose, M.; Yoneda, Y.; Sano, M. "The Third Phase" of Extraction Process in Fuel Reprocessing, (II) Exafs Study of Zirconium Monobutylphosphate and Zirconium Dibutylphosphate. *J Nucl Sci Technol* **1990**, *27* (3), 256–261. https://doi.org/10.1080/18811248.1990.9731177.

(53) Miyake, C.; Hirose, M.; Yoshimura, T.; Ikeda, M.; Imoto, S.; Sano, M. "The Third Phase" of Extraction Processes in Fuel Reprocessing, (I): Formation Conditions, Compositions and Structures of Precipitates in Zr-Degradation Products of TBP Systems. *J Nucl Sci Technol* **1990**, *27* (2), 157–166. https://doi.org/10.1080/18811248.1990.9731164.

(54) Lefebvre, C.; Dumas, T.; Tamain, C.; Ducres, T.; Solari, P. L.; Charbonnel, M. C. Addressing Ruthenium Speciation in Tri-n-Butyl-Phosphate Solvent Extraction Process by Fourier Transform Infrared, Extended X-Ray Absorption Fine Structure, and Single Crystal X-Ray Diffraction. *Ind Eng Chem Res* **2017**, *56* (39), 11292–11301. https://doi.org/10.1021/acs.iecr.7b02973.

(55) Antonio, M. R.; Ellis, R. J.; Estes, S. L.; Bera, M. K. Structural Insights into the Multinuclear Speciation of Tetravalent Cerium in the Tri-n-Butyl Phosphate-n-Dodecane Solvent Extraction System. *Physical Chemistry Chemical Physics* **2017**, *19* (32), 21304–21316. https://doi.org/10.1039/c7cp03350h.

(56) Tkac, P.; Paulenova, A. Spectroscopic Identification of Tri- n -Butyl Phosphate Adducts with Pu(IV) Hydrolyzed Species . *IOP Conf Ser Mater Sci Eng* **2010**, *9* (Iv), 012072. https://doi.org/10.1088/1757-899x/9/1/012072.

Curriculum Vita

Jonathan George

georgejonathaan@gmail.com

EDUCATION

Master of Science, Chemistry – Focus in Radiochemistry
August 2021 – Present

University of Nevada, Las Vegas | Las Vegas, NV

Thesis – INTERACTION OF TECHNETIUM(IV) WITH DIBUTYL PHOSPHATE IN n-DODECANE

Bachelor of Science, Chemistry

University of Nevada, Las Vegas | Las Vegas, NV
August 2014 – December 2019

RELEVANT COURSES

HPS 601 Nuclear Physics

HPS 602 Radiation Detection

RDCH 702 Radiochemistry

RDCH 710 Actinide Chemistry I & II

RDCH 750 Radiochemistry Laboratory Research

CHEM 793 Electrochemistry

CHEM 793 Advanced Radiochemistry Methods

CHEM 793 Molten Salt Chemistry

CHEM 793 Nuclear Forensics

EXPERIENCE

August 2021 – Present | Las Vegas, NV

Graduate Research Assistant, Radiochemistry Program, University of Nevada, Las Vegas

Primary Investigators: Dr. Frederic Poineau & Dr. Artem V. Gelis

- Perform kinetic studies of pertechnetate ions reduced by hydrazine in a nitric acid media.
- Conduct electrochemical studies of reduced pertechnetate ions in aqueous and organic media.
- Develop solvent extraction and scintillation techniques for calculating extraction coefficients and total ^{99}Tc concentrations.
- Prepare and analyze concentrated Th and Tc samples for x-ray absorption spectroscopy.
- Repair and support Radiochemistry Program instrumentation.
- Present work and prepare manuscripts for peer-reviewed publications.

Summer 2022 | Livermore, CA

Intern, Additive Manufacturing Laboratory, Lawrence Livermore National Laboratory

Primary Investigators: Mr. Dominque Porcincula & Dr. Jason Brodsky

- Formulated various resin compositions with a range of concentrations for primary and secondary dyes to support the manufacturing of plastic scintillators.
- Performed UV-Vis. and fluorescence spectroscopy measurements of formulated resins.
- 3D printed plastic scintillator material using stereolithography techniques.
- Utilized light output techniques for comparing against industry standard EJ200.

Summer 2020 | San Antonio, TX

Postbaccalaureate Research Assistant, Consortium on Nuclear Security Technologies, University of Texas, San Antonio

Primary Investigator: Dr. Elizabeth Sooby

- Simulated defect formation energies of zirconium within a U_3Si_2 framework in various interstitial and substitutional positions.
- Drafted manuscripts for peer-reviewed publications.

March 2017 – August 2021 | Las Vegas, NV

Undergraduate Research Assistant, Radiochemistry Program, University of Nevada, Las Vegas

Primary Investigators: Dr. Kenneth Czerwinski & Dr. Eunja Kim

- Dissolution and analysis of uranium oxides in ionic liquid (TFSI/MPPI) and electrodeposition on Au electrodes.
- Alloyed and analyzed burnup metallic fuel systems (^{238}U, Lanthanides) using STA (TGA & DSC) methods.
- Synthesized and studied U and Tc oxides and ceramic waste form ($^{238,233}U$, ^{99}Tc) morphology and crystallography via SEM and PXRD.
- Simulated double periodate and cesium-bearing ceramic waste forms using Density Functional Theory.

RADIONUCLIDE EXPERIENCE

- **^{99}Technetium:** $(NH_4, K, Tl)TcO_4$, TcO_2, Tc(0)
- **^{237}Neptunium:** NpO_2, $Np(OH)_5$, $NpO_3 \cdot H_2O$
- **^{233}Uranium:** UO_2^{2+}, UO_3
- **^{238}Uranium:** UO_x [x=2,3], U_3O_8, $(NH_4, Li, Cs)_2U_2O_7$, $UO2(NO_3)_2$, UF_y [y=4,6], UI_3, U(0)

INSTRUMENTATION & TECHNIQUES

- Alpha Spectroscopy
- Arc Melting
- Density Functional Theory (VASP)
- Differential Scanning Calorimetry
- Fluorescence Spectroscopy
- Gamma Spectroscopy
- Inert Atmosphere Gloveboxes
- Large-Area Projection Micro-Stereolithography
- Liquid-Liquid Extraction
- Liquid Scintillation Counting
- Nuclear Magnetic Resonance
- Potentiometry
- Powder X-Ray Diffraction
- Real-Time Fourier Transform Infrared Spectroscopy
- Scanning Electron Microscopy
- Thermogravimetric Analysis
- Ultraviolet-Visible Spectroscopy
- X-ray Absorption Spectroscopy

PUBLICATIONS & PRESENTATIONS

- **George, J.**, Poineau, F. (2022, Oct). "The nature of technetium in spent nuclear fuel", Environmental Chemistry, Energy Storage, Education Poster Session. American Chemical Society Western Regional Meeting. Las Vegas, NV.
- Louis-Jean, J., **George, J.**, & Poineau, F. (2022). "From ammonium hexahalorhenates (IV) to nanocrystalline rhenium metal: A combined thermal, diffraction and microscopic analysis," *IJRMHM*, *105*, 105840.
- Moczygemba, C., **George, J.**, Montoya, E., Kim, E., Robles, G., & Sooby, E. (2022). Structure Characterization and Steam Oxidation Performance of U_3Si_2 with Zr Alloying Additions," *J. Nuc. Mat*., 153951.
- O'Sullivan, S.E., Montoya, E., Sun, S.-K., **George, J.**, Kirk, C., Dixon-Wilkins, M.C., Weck, P.F., Kim, E., Knight, K.S., Hyatt, N.C. Hyatt. (2020). "Crystal and electronic structures of A2NaIO6 periodate double perovskites (A= Sr, Ca, Ba): candidate wasteforms for I-129 immobilization," *Inorg. Chem*.,
-

PROFESSIONAL MEMBERSHIP

American Nuclear Society (ANS)

Education Outreach Chair | Jan 2020 – Jan 2021

Connect and travel to high schools in the Las Vegas valley to stimulate and educate about on nuclear sciences and topics.

General Member | Jan 2019 – Aug 2023

Active in UNLV chapter to discuss general topics related to nuclear technology, safeguards, and sciences. Provide outreach events for local youth to learn about nuclear sciences.

AWARDS & ACHIEVEMENTS

Minority Serving Institute Internship Program (MSIIP) Internship (*2022)*

Consortium on Nuclear Security Technologies Research Experience (*2020 – Present)*

Governor Guinn Millennium Scholarship (2014)